9-12-2014

Efficient Multiphysics Coupling for Fast Burst Reactors in Slab Geometry

Japan Patel

Follow this and additional works at: https://digitalrepository.unm.edu/ne_etds

Recommended Citation

_____

Candidate

_____

Department

This thesis is approved, and it is acceptable in quality and form for publication:

Approved by the Thesis Committee:

_____ , Chairperson

_____

_____

_____

_____

_____

_____

EFFICIENT MULTIPHYSICS COUPLING FOR FAST BURST REACTORS IN SLAB GEOMETRY

BY

JAPAN KETAN PATEL

HONORS B. S., NUCLEAR ENGINEERING, OREGON STATE UNIVERSITY, 2011

THESIS

Submitted in Partial Fulfillment of the
Requirement for the Degree of

Master of Science

Nuclear Engineering

The University of New Mexico
Albuquerque, New Mexico

July, 2014

Acknowledgements

At this point, I would like to thank Dr. Cassiano de Oliveira for his infinite patience and support. I am grateful to him for making me an independent researcher. His insights on multiphysics modeling have been invaluable. I would like to thank Dr. Hyeongkae Park for teaching me almost everything that went into this thesis. It is, really, his ideas that have been executed in this thesis. I thank Dr. Salvador Rodriguez for teaching the CFD class, being on my committee, going through my thesis, and important edits inspite of bad health. I would also like to thank Dr. Anil Prinja for various discussions over the last year that proved to be helpful in understanding the subject matter. I thank my thesis committee – Dr. Cassiano de Oliveira, Dr. Hyeongkae Park, Dr. Anil Prinja, and Dr. Salvador Rodirguez for being on my thesis committee.

I thank Ms. Jocelyn White, and Mr. Doug Weintraub, for helping me with all the paperwork.

I owe everything to my parents. Thank you, Mohna and Ketan Patel.

EFFICIENT MULTIPHYSICS COUPLING FOR FAST BURST REACTORS IN SLAB GEOMETRY

BY

JAPAN KETAN PATEL

HONORS B. S., NUCLEAR ENGINEERING, OREGON STATE UNIVERSITY, 2011

ABSTRACT OF THESIS

Submitted in Partial Fulfillment of the
Requirement for the Degree of

Master of Science

Nuclear Engineering

The University of New Mexico
Albuquerque, New Mexico

July, 2014

EFFICIENT MULTIPHYSICS COUPLING FOR FAST BURST REACTORS IN SLAB GEOMETRY

by

Japan Ketan Patel

Honors B. S., Nuclear Engineering, Oregon State University

M. S., Nuclear Engineering, University of New Mexico

ABSTRACT

In this thesis, we discuss a coupling algorithm to model simplified fast burst reactor dynamics. Kadioglu presented a tightly coupled multiphysics algorithm of diffusion neutronics and linear. An implicit-explicit (IMEX) algorithm was used to follow the dynamical time-scale of the problem. However, as noted by Kadioglu and his co-authors, the diffusion model does not adequately represent the neutronics of the system due to its small. Our objective is to extend the IMEX algorithm to incorporate transport effects using moment based acceleration concept. We will demonstrate the differences between diffusion and transport models (S_N). We will also demonstrate how the introduction of moment based acceleration enables us to isolate the angular flux from coupled multiphysics system by using a discretely consistent lower order (LO) system.

Table of Contents

Chapter 1: Introduction

Fast burst reactors are highly enriched uranium/plutonium, unshielded, pulsed reactors that produce bursts of neutrons and photons to irradiate test samples (Shabalin, 1979). These reactors rely on natural thermo-mechanical properties to turn on (supercritical) and off (subcritical) (Burgreen, 1962). We are interested in accurately modeling this transition of the reactor from supercritical to subcritical and the corresponding material response with a novel multiphysics, multiscale algorithm.

Following the evolution of such systems involves adequately accurate prediction of flux, temperature, and displacement fields over time. In this thesis, we use one group, slab geometry neutron transport model (S_N) with isotropic scattering to predict the flux distribution. We neglect delayed neutrons since the physical time-scales of interest are too small for delayed neutrons to have any substantial bearing. We use the linear elasticity model to approximate material feedback, and the adiabatic heat-up model to approximate the temperature evolution of the system. We do not account for heat conduction, convection or radiation cooling in the adiabatic heat-up model. We also note that our study is limited to very small reactivity insertions so that linear mechanics model can adequately model the system.

This study extends the IMEX algorithm from (Kadioglu et al., 2009) is extended to include transport effects. We note that the transport sweeps can be expensive so isolating the transport solver from the coupled multiphysics system is of interest. Therefore, we also introduce moment based acceleration concept into our transport model and evaluate its performance. We use centered finite difference spatial discretization throughout this thesis.

Additional motivation for this work comes from our interest in modeling the fast pulsed and burst reactor systems in full 3D geometry with nonlinear mechanics. This thesis will serve as a stepping stone towards that goal.

1.1 Governing Equations

We use the following one-group slab geometry neutron balance equation with isotropic scattering to model the evolution of the neutron population:

$$\frac{1}{\vartheta}\frac{\partial \Phi}{\partial t} + \frac{\partial J}{\partial x} + \Sigma_a \Phi = v\Sigma_f \Phi. \tag{1}$$

Here, $\Phi(x,t)$ and $J(x,t)$ are the scalar flux and current respectively at position x and time t. Σ_a is the macroscopic absorption cross section, Σ_f is the macroscopic fission cross section, v is the average number of neutrons produced per fission, ϑ is the neutron velocity. Eq. 1 can also be viewed as the zeroth angular moment of the following transport equation:

$$\frac{1}{\vartheta}\frac{\partial \psi}{\partial t} + \mu\frac{\partial \psi}{\partial x} + \Sigma_t \psi = \frac{1}{2}(\Sigma_s + v\Sigma_f)\,\Phi. \tag{2}$$

Here, $\psi(x, \mu, t)$ is the angular flux, Σ_s is the macroscopic scattering cross section, and Σ_t is the macroscopic total cross section.

In addition, when we employ Fick's law, we can rewrite Eq. 1 as the following diffusion equation:

$$\frac{1}{\vartheta}\frac{\partial \Phi}{\partial t} - \frac{\partial}{\partial x}D\frac{\partial \Phi}{\partial x} + \Sigma_a \Phi = v\Sigma_f \Phi. \tag{3}$$

Here, D is the diffusion coefficient.

The macroscopic cross section, Σ, is a function of the number density, which in turn, depends on the material density. The material density can be evaluated using simple mass conservation,

$$\rho = \rho_0 \left(\frac{x}{x+u}\right)^3. \tag{4}$$

Here, ρ is the density and u is the material displacement.

To model the material displacement, we use the following linear elastic wave equation (Reuscher, 1969):

$$\frac{1}{c^2}\frac{\partial^2 u}{\partial t^2} = \frac{\partial^2 u}{\partial x^2} - \frac{\alpha(1+\sigma)}{(1-\sigma)}\frac{\partial T}{\partial x} \tag{5}$$

with,

$$c^2 = \frac{E(1-\sigma)}{(1+\sigma)(1-2\sigma)\rho}. \tag{6}$$

Here, c, α, σ and E are wave speed, linear thermal expansion coefficient, Poisson's ratio, and Young's modulus respectively. T is the material temperature. As in (Kadioglu et al., 2009), we note that while linear elasticity (linear mechanics) model may accurately solve for small material displacements, it may not be adequate to model large displacements. We would need nonlinear mechanics – hydrodynamics equations – to solve for large material displacements. Therefore, our study is limited to very small reactivity insertions only.

Finally, we use the following adiabatic heat-up model for the evolution of temperature field:

$$\rho c_p \frac{\partial T}{\partial t} = \omega \Sigma_f \Phi. \tag{7}$$

Here, c_p is the specific heat and ω is the average heat produced per fission.

Note the lack of heat removal mechanism in Eq. 7. This will have its bearing on the model. We will see that the reactor will expand and reach a new (expanded) equilibrium state without returning to its original state because of this. More will be said about multiphysics modeling of the slab geometry FBR in later sections of this thesis.

We will, now, take a quick detour and look at the work that has already been done in transport acceleration, multiphysiscs modeling involving neutron transport, and FBR modeling.

1.2 Literature Review

In this section we will discuss the work done on acceleration of source iteration. We will also discuss work done in multiphysics modeling with transport. Finally, we will discuss the work that has been done in FBR modeling.

(Prinja et al., 2010) derives the general transport equation and then simplifies it to one group, slab geometry equation with isotropic scattering. We discuss the discrete ordinates method and its acceleration for this slab geometry transport model only since this thesis deals with slab geometry model. Eq. 2 represents the transient, one group transport equation in slab geometry.

We have three independent variables – temporal position, spatial position, and angular cosine. We discretize the equation in space using the centered finite difference scheme, also known as the diamond difference. We use the discrete ordinates (S_N) method to discretize angle, and backward difference methods - first order backward difference (BDF1) and second order backward difference (BDF2) to discretize time. The time dependent transport equation used in this study takes the following form with discrete ordinated angular discretization:

$$\frac{1}{\vartheta}\frac{\partial\psi(x,\mu_j)}{\partial t} + \mu_j\frac{\partial\psi(x,\mu_j)}{\partial x} + \Sigma_t\psi(x,\mu_j) = \frac{1}{2}(\Sigma_s + v\Sigma_f)\sum_{j=1}^{N} w_j\psi(x,\mu_j) \tag{8}$$

Note that the above equation is not directly invertible and an iterative method must be employed to solve it. The simplest of these methods is the Richardson iteration method where we guess an initial angular flux profile and then iterate over the source until convergence to obtain the flux profile. This method is also called source iteration. This standard method has been described at length in (Bell et al., 1979). Source iteration has a physical significance as each iteration accounts for one scatter plus fission. Thus in a medium with high scatter and fission, we expect higher number of iterations and therefore, slow convergence.

4

There have been several studies in which different methods have been employed to accelerate source iteration. Some of these methods include linear techniques like diffusion synthetic acceleration (DSA), transport synthetic acceleration (TSA), KP synthetic acceleration, Lewis and Miller methods (LM), and multigrid methods, and nonlinear acceleration techniques like quasi-diffusion (QD), nonlinear diffusion acceleration (NDA) and weighted alpha methods (WA). Some other methods include rebalance methods, boundary projection acceleration (BPA), asymptotic source extrapolation (ASE), Chebychev acceleration, and Conjugate Gradient acceleration methods as discussed in by Adams and Larsen in (Adams et al., 2002).

The source iteration method is iterative; therefore, the convergence depends on suppression of error modes. While source iteration effectively suppresses error modes with strong angular and spatial dependence, it doesn't effectively suppress error modes with weak angular and spatial dependence. Acceleration techniques, essentially, attempt to suppress these slowly vanishing error modes. Linear acceleration methods do that using additive correction term, while nonlinear methods do that using multiplicative term (Adams et al., 2002). Each acceleration method starts with a transport sweep (one source iteration) of the higher order (HO) transport equation followed by calculation of the correction using the lower order (LO) equation. This LO equation differs with different acceleration techniques. DSA, for example, uses diffusion equation for calculation of the correction, while TSA uses the transport equation. There may be additional, supplemental steps that one may take in order to obtain highly accurate correction terms, as in the case of KP methods (Adams et al., 2002).

Kopp presented the idea of synthetic acceleration in (Kopp, 1963). Levedev presented his KP synthetic acceleration technique in (Lebedev, 1964) and (Lebedev, 1967). Marchuk and Lebedev discussed the KP methods, and its convergence at length in (Marchuk et al., 1986). Later, Gelbard and Hageman came up with their study that used diffusion and S_2 as the lower order equations for

synthetic acceleration in (Gelbard, 1969). It was later discovered by Reed in (Reed, 1971) that Gelbard and Hageman's synthetic acceleration technique diverged on coarse grids. Alcouffe presented his DSA method that fixed the divergence issue (Alcouffe, 1976) by introducing discrete consistency between the HO and LO equation discretization. Gol'din presented his idea of quasidiffusion in (Gol'din et al., 1964). Larsen and Anistratov described their WA methods in (Anistratov et al., 1995). Larsen presented his multigrid (2 grids) acceleration technique in (Larsen, 1990). Multiple other multigrid techniques were presented in (Nowak et al., 1987), (Nowak et al., 1988), (Barnett et al., 1989), etc. The notion of TSA was described by Ramone, Adams and Nowak in (Ramone et al., 1997) where transport sweep was used as the LO correction equation. LM first and second moment schemes were proposed by Lewis and Miller in (Lewis et al., 1976) where the correction is obtained using the P_1 equation. A nonlinear version of first moment LM scheme was presented recently by Smith and Rhodes in (Smith et al., 2000). The review paper by Adams and Larsen (Adams et al., 2002) describes several prominent acceleration techniques and points to all of the above cited references along with several others. They also present how the synthetic methods may be viewed as preconditioned source iteration methods.

Knoll, Park, and Smith applied the Jacobian-free Newton Krylov (JFNK) method to nonlinear acceleration of transport to slab geometry problems in (Knoll et al., 2011). They also present the effect of two grid approach on iteration convergence. In (Park et al., 2012), Park, Knoll, and Newman present a nonlinear acceleration method for the transport criticality problem. Both of these papers are used extensively in our multiphysics model as will be seen in the coming chapters.

Multiple studies have looked into coupling neutron transport with other physics. We will look at some of the coupling techniques at length in Appendix D. Some of the papers on integration of radiation transport into multiphysics algorithms will be cited in this section. Seker, Thomas and Downar present a multiphysics algorithm that integrates transport and fluid dynamics via coupling

MCNP5 and STAR-CD in (Seker et al., 2007). Their code coupling method uses Picard iteration to converge on flux. Procassini, Chand, Clouse, Ferencz, Grandy, Henshaw, Kramer, and Parsons present their report on OSIRIS code that incorporates coupling for stand-alone thermal-hydraulics and monte-carlo neutronics legacy codes in (Procassini, 2007). OSIRIS employs loose coupling to couple relevant physics. Lockwood presents a coupling algorithm where he couples conjugate heat transfer with neutronics in (Lockwood, 2007). He used loose coupling between even parity transport code, EVENT for neutronics and his independent implementation of Pressure-Corrected Implicit Continuous Eulerian (PCICE) algorithm. Park, Knoll, Gaston, and Martineau present a fully implicit multiphysics algorithm to solve coupled thermal-fluid and neutronics problems in (Park et al., 2010). They demonstrate the application of their algorithm to modeling pebble bed reactors. Tamang presents a coupling algorithm to couple transport with quasi diffusion LO equation and grey approximation with heat transfer in (Tamang, 2013). He uses Richardson iteration in order to solve for flux.

FBRs have been studied extensively in the past. In 1969, several papers were presented at the National Topical Meeting on Fast Burst Reactors, Albuquerque. McTaggart presented on fast burst reactor kinetics where he reviewed methods of deriving reactivity feedback in terms of one point model with separable time and space dependence (McTaggart, 1969). Reuscher presented on thermomechanical analysis of fast burst reactors where the thermomechanical aspects of the reactor were discussed without coupling with neutronics in (Reuscher, 1969). Several papers were again presented on pulse reactors at the Topical Meeting on Physics, Safety, and Applications of Pulse Reactors in 1994. Hetrick, Kimpland, and Kornreich presented a model coupling point kinetics, equation of state for liquid containing radiolytic gas bubbles and equations for fluid acceleration to computationally model homogeneous water solution pulse reactors in (Hetrick et al., 1994). Pasternoster, Kimpland, Jaegers, and McGhee presented a fully coupled neutronics (point kinetics)-hydrodynamic response of fast burst reactors under disruptive accident conditions in

(Paternoster, 1994). Wilson, Biegalski, and Coats coupled Nordheim-fuchs kinetics equations and thermoelasticity equations to study the behavior of Godiva like nuclear assemblies in (Wilson et al., 2007). Green coupled multigroup diffusion equation with heat transfer and thermoelasticity models to simulate reactor pulses in fast burst and externally drive nuclear assemblies in (Green, 2008). Kadioglu, Knoll, and de Oliveira presented an implicit-explicit algorithm to couple diffusion, heat transfer, and material energy equations in order to model fast burst reactors in (Kadioglu et al., 2009). This thesis is a natural extension of this same paper by Kadioglu et al.

Chapter 2: Multiphysics Coupling

In this chapter, we introduce the basic concept of multiphysics and multiphysics coupling in numerical modeling. In the following subsections, we will look at what multiphysics is and different classes of multiphysics systems. We will also look at numerical techniques that can be used to solve such systems. Towards the end of this chapter, we will demonstrate how we specifically couple the physics related to our FBR problem and present the solution algorithm that will be at the core all further study in this thesis.

2.1 Introduction to Multiphysics

Most systems are made of interactive subsystems. This interaction of the subsystem often dictates the overall behavior of the system. Therefore, in order to accurately model the overall behavior of systems, we must accurately model the interaction between relevant subsystems along with the evolution of these subsystems themselves. In numerical modeling, it is this collective modeling of individual subsystems and their interactions that is termed as multiphysics modeling.

According to (Keyes et al., 2012), there are multiple ways to classify multiphysics systems. One way to classify them is by region, i.e. whether the coupling occurs in bulk region (bulk coupled) or just at interfaces (interface coupled). Examples of bulk coupled multiphysics systems include radiation-hydrodynamics, magneto-hydrodynamics, reactive transport, temperature feedback in nuclear reactors etc. The FBR system under study in this thesis falls under this class of multiphysics problems. Examples of interface-coupled multiphysics problems include ocean-atmosphere dynamics, and fluid-structure interactions among others. Another class of multiphysics problems is that of problems that are inherently multiscale, where the same phenomena are described by multiple formulations with a specific transition region or boundary. An example of such multiscale phenomena is that of crack propagation in solids where atomistic and continuum models are both hold in respective regimes. Yet another class of multiphysics problems is that of multi-rate or multi-

resolution problems. Other classes of multiphysics problems include systems of partial differential equations that include equations of different types and the ones with different discretization for the same physical model.
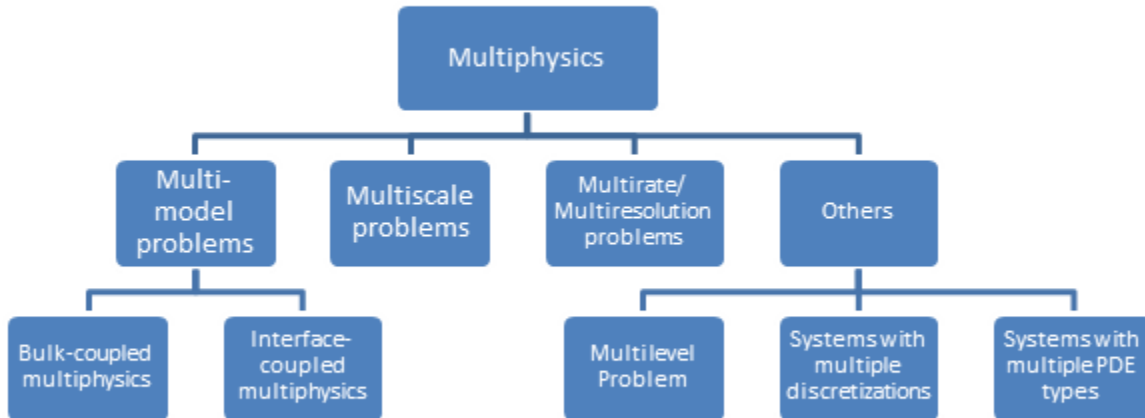
**Figure 1: Multiphysics Classification**

Each class of multiphysics problems, whether multiscale, multirate, multilevel, or multimodel, include partitioning of the overall system into subparts or subsystems that evolve through a sequence of updates of dependent variables (Keyes et al., 2012). More details on each class of the multiphysics problems can be found in (Keyes et al. 2012). The evolution of these problems, however, depends heavily on how the subsystems interact. That is discussed in the next subsection on multiphysics coupling.

2.2 Introduction to Coupling

Coupling describes how the subsystems of the multiphysics systems interact. The coupling can be classified into one-way coupled and two-way coupled problems depending on how subsystems

depend on each other. A one-way coupled system typically consists of a system of equations with only forward or backward dependence. In other words, the system of equations is linearly coupled and can be solved in a sequential manner. Two-way coupled systems consist of systems of equations with both forward and backward dependence. These are non-linearly coupled systems and require nonlinear iteration for their solution. Nonlinearly coupled systems may further be classified into different classes depending on the solution strategy. The coupling may be tight or loose. Loosely coupled systems typically arise out or a Gauss Seidel type or an operator split type solution strategy. Picard iteration is predominantly used here. Tight coupling results from Newton type solve (Keyes et al., 2012).

The following figure summarizes different classes of multiphysics coupling:
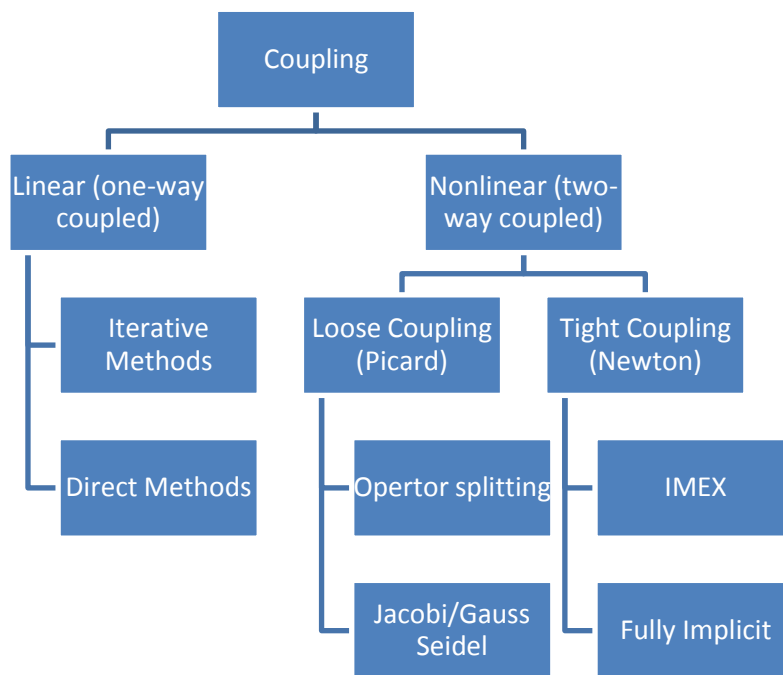
Figure 2: Multiphysics Coupling

As in (Keyes et al., 2012), we will now look at the three major multiphysics coupling methods. Consider a generic coupled problem with two residual functions:

$$R_1(a, b) = 0 \tag{9}$$

$$R_2(a, b) = 0 \tag{10}$$

In order to model the coupled system of Eq. (9) and Eq. (10), we may typically employ three different strategies:

Gauss Seidel Method: This is the most widely used multiphysics coupling strategy. It preserves the integrity of each subsystem where it solves respective subsystems separately, sequentially, and then iterates until desired convergence is observed. The following algorithm describes this type of coupling.

Gauss Seidel Coupling (Keyes et al., 2012):

1) Supply initial fields, $[a^0]$ and $[b^0]$.
2) Start a while loop until convergence with iteration index g.
3) Compute x in $R_1(x, b^{g-1}) = 0$.
4) Set $a^g = x$.
5) Compute y in $R_2(a^g, y) = 0$.
6) Set $b^g = y$.
7) Loop back
8) Loop over to the next time step if the process is transient.

These types of algorithms result in loose coupling.

Operator Splitting: Time evolution problems often utilize operator splitting methods in time. The following algorithm describes how a generic operator splitting method works.

Operator Split Coupling (Keyes et al., 2012):

1) Supply initial fields, $[a^0]$ and $[b^0]$.

2) Start time loop with iteration index, t.

3) March in time with $R_1(a, b_{t-1}) = 0$ to compute a_t.

4) March in time with $R_2(a_t, b) = 0$ to compute b_t.

5) Loop back to the next time step.

Each individual time march in the above algorithm may be implicit or explicit. We may or may not have within time-march iterations known as subcycling to obtain better quality solutions. We may also stagger the solution in time. The above algorithm results in first order time splitting errors which renders the solution first order accurate inspite of using higher order discretization schemes. Higher order operator schemes like Strang splitting and temporal Richardson extrapolation must be used to obtain higher order solution accuracy for the coupled system while using operator split coupling technique (Keyes et al., 2012). This method of coupling also results in loose coupling.

Newton Method: As per (Keyes et al., 2012), this method takes into account all the subsystems of the multiphysics model and formulates a single residual function. In other words,

$$R(a, b) = \begin{bmatrix} R_1(a, b) \\ R_2(a, b) \end{bmatrix} = 0. \tag{11}$$

Let $(a, b) = u$. The Jacobian of the equation system is given by

$$\mathbb{J} = \begin{bmatrix} \dfrac{\partial R_1}{\partial a} & \dfrac{\partial R_1}{\partial b} \\ \dfrac{\partial R_2}{\partial a} & \dfrac{\partial R_2}{\partial b} \end{bmatrix} \tag{12}$$

The following algorithm is used for Newton solve of the multiphysics system.

Newton's Method (Keyes et al., 2012):

1) Supply initial field u^0.

2) Start a while loop for convergence with iteration index, k.

3) Compute correction δu, using $\mathbb{J}(u^{k-1})\delta u = -R(u^{k-1})$.

4) Update $u^k = u^{k-1} + \delta u$.

5) Loop back.

6) Loop back to the next time step for transient problems.

Newton's method results in tight coupling. The Newton system in step 3 of the above algorithm can be solved by multiple different methods (Kelley, 2003). We can employ direct methods or iterative methods to solve that system. Sometimes, however, calculating the exact Jacobian becomes quite tedious in which case, Jacobian Free Newton-Krylov (JFNK) method becomes very useful (Knoll et al., 2002).

Now that we've seen the three basic coupling schemes, we move on to the next subsection where we will describe the coupling scheme to be used for modeling the FBR problem. We will also discuss Newton's method in more detail.

2.3 FBR Coupling Scheme

The coupled FBR system can be solved iteratively using Newton's method (Kelley, 2003). Newton's method iteratively finds the solution $\boldsymbol{U}$ that satisfies the relevant nonlinear residual functions,

$$F(\boldsymbol{U}) = 0. \tag{13}$$

Here, F is the nonlinear residual function. In our FBR system, $F = [F_u, F_\Phi, F_T]^T$, and $\boldsymbol{U} = [u, \Phi, T]^T$. In order to solve Eq. 13, Newton's method utilizes Taylor series expansion,

$$F(\boldsymbol{U}) \approx F(\boldsymbol{U_m}) + \delta\boldsymbol{U} \frac{\partial F}{\partial U}|_{U_m}. \tag{14}$$

Rearranging the above equation yields,

$$\mathbb{J}_m \delta U \approx -F(U_m) \tag{15}$$

where,

$$\mathbb{J}_m = \left. \frac{\partial F}{\partial U} \right|_{U_m} \tag{16}$$

is the Jacobian matrix. Specifically, in our FBR system, the Newton system can be represented as following:

$$\begin{pmatrix} \mathbb{J}_{uu} & \mathbb{J}_{u\Phi} & \mathbb{J}_{uT} \\ \mathbb{J}_{\Phi u} & \mathbb{J}_{\Phi\Phi} & \mathbb{J}_{\Phi T} \\ \mathbb{J}_{Tu} & \mathbb{J}_{T\Phi} & \mathbb{J}_{TT} \end{pmatrix} \begin{bmatrix} \delta u \\ \delta \Phi \\ \delta T \end{bmatrix} = - \begin{bmatrix} F_u \\ F_\Phi \\ F_T \end{bmatrix}. \tag{17}$$

Moreover, the residual functions can be represented as follows:

$$F_u = \frac{1}{c^2} \frac{\partial^2 u}{\partial t^2} - \frac{\partial^2 u}{\partial x^2} + \frac{\alpha(1+\sigma)}{(1-\sigma)} \frac{\partial T}{\partial x}, \tag{18}$$

$$F_\Phi = \frac{1}{\vartheta} \frac{\partial \Phi}{\partial t} - \frac{\partial}{\partial x} D \frac{\partial \Phi}{\partial x} + \Sigma_a \Phi - \upsilon \Sigma_f \Phi, \tag{19}$$

$$F_T = \rho c_p \frac{\partial T}{\partial t} - \omega \Sigma_f \Phi. \tag{20}$$

We see that due to no direct dependence of the displacement on scalar flux and scalar flux on temperature, the Newton system can be reduced to the following:

$$\begin{pmatrix} \mathbb{J}_{uu} & 0 & \mathbb{J}_{uT} \\ \mathbb{J}_{\Phi u} & \mathbb{J}_{\Phi\Phi} & 0 \\ \mathbb{J}_{Tu} & \mathbb{J}_{T\Phi} & \mathbb{J}_{TT} \end{pmatrix} \begin{bmatrix} \delta u \\ \delta \Phi \\ \delta T \end{bmatrix} = - \begin{bmatrix} F_u \\ F_\Phi \\ F_T \end{bmatrix}. \tag{21}$$

Thus far, we have not assumed any specific temporal discretization. In many cases, the implicit time discretization can be advantageous because implicit methods allow one to choose the time step size from an accuracy perspective, and not stability perspective. In the FBR system, the dynamical time scale of the problem is closely related to the characteristic wave speed of the material displacement (linear mechanics equation). Therefore, the implicit-explicit (IMEX) scheme developed by Kadioglu et al. (Kadioglu et al., 2009) which solves Eq. 5 explicitly and Eq. 1, and Eq. 7 implicitly can be utilized. Assuming explicit temporal discretization for linear mechanics, Eq. 17 is further reduced to the following lower block triangular matrix:

$$
\begin{pmatrix} \mathbb{J}_{uu} & 0 & 0 \\ \mathbb{J}_{\Phi u} & \mathbb{J}_{\Phi\Phi} & 0 \\ \mathbb{J}_{Tu} & \mathbb{J}_{T\Phi} & \mathbb{J}_{TT} \end{pmatrix} \begin{bmatrix} \delta u \\ \delta\Phi \\ \delta T \end{bmatrix} = - \begin{bmatrix} F_u \\ F_\Phi \\ F_T \end{bmatrix}. \tag{22}
$$

At the same time we also note that time step size required to solve neutronics equations explicitly would be impractically small due to the stiffness of the problem. Therefore, we solve the neutronics equation implicitly. This combination of implicit neutronics and material energy, and explicit linear mechanics yields the IMEX scheme (Kadioglu et al., 2009) to solve the coupled system.

Notice that with the introduction of explicit linear mechanics (instead of implicit) this system becomes one way coupled. This can be verified from the fact that we get a block lower triangular Jacobian matrix. This allows us to solve the coupled system in a sequential way where we solve for the displacement first, then solve for flux, and then the temperature for each time. The implementation of the IMEX scheme makes the coupling linear, therefore, we do not iterate between physics.

We utilize the following IMEX algorithm:

1. Initialize variables and declare parameters. Use the eigenvalue problem to initialize flux, and amplify it so that the power in the system is approximately unity.

16

2. March the **explicit** linear mechanics equation in time to calculate the displacement profile.

3. Calculate resultant density change and update density.

4. Update cross sections resulting from change in density.

5. March the **implicit** neutronics equation to calculate a new flux profile.

6. March the **implicit** temperature equation to calculate a new temperature profile

7. Loop back for next time step.

Chapter 3: Modeling the FBR System

In this chapter, we solve the FBR problem using diffusion, and transport (S_N) neutronics. First, we model the system with diffusion neutronics. Then we present the motivation for extension to transport neutronics and compare the results from diffusion and transport neutronics.

3.1 Model System

Reactor System

This study uses a slab reactor which is symmetric about its center. Thus we model a half slab of ^{239}Pu of length 0.07665 [m] with its center being on the left boundary. Figure 1 presents a pictorial representation of the reactor system.

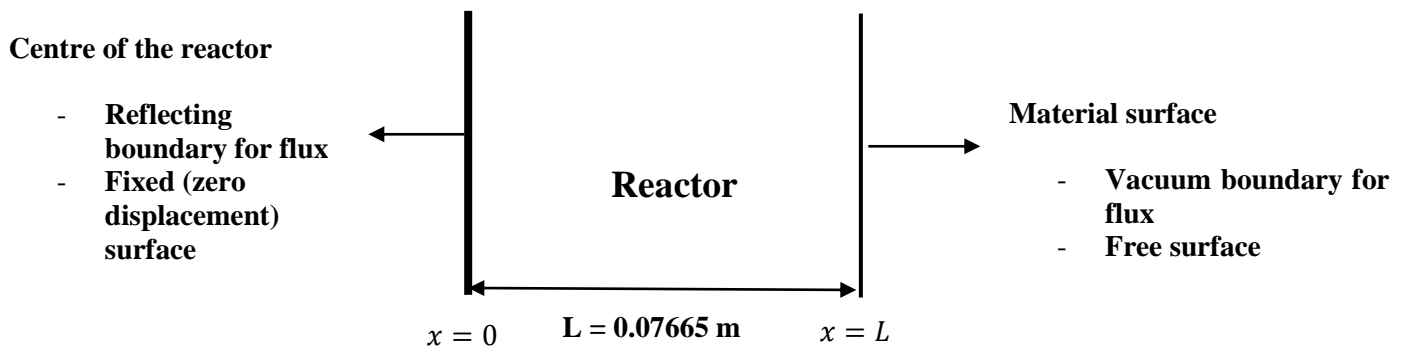**Centre of the reactor**

- **Reflecting boundary for flux**
- **Fixed (zero displacement) surface**

Reactor

Material surface

- **Vacuum boundary for flux**
- **Free surface**

$x = 0$ **L = 0.07665 m** $x = L$

Figure 3: Model Reactor System

The material parameters of the reactor system are as follows. Number density is 4.938×10^{28} [atom/m^3]. The neutron velocity is 1×10^7 [m/s]. The microscopic total cross section, microscopic absorption cross section, and microscopic fission cross section for the system are 6.8×10^{-28} [m^2], 2.11×10^{-28} [m^2], and 1.85×10^{-28} [m^2] respectively. The specific heat capacity of the system is 130 [J/kgK]. The atomic mass is 399.13×10^{-27} [kg/atom], while the mass density is 19.709×10^3 [kg/m^3]. The Poisson ratio, Young's modulus, and linear thermal expansion coefficient are 0.15, 1×10^{11} [Pa], and 53×10^{-6} [1/K] respectively.

Discretization: The grid used for this problem is as follows:
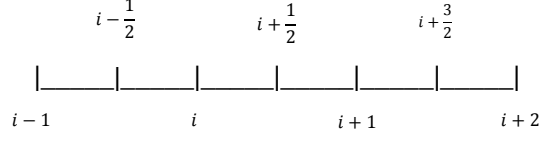
Figure 4: Grid Indexing

Here, i goes from 1 to I, where I is the number of nodes.

Throughout this study, we use subscript i for the nodal index and $i \pm \frac{1}{2}$ for cell centered/averaged values.

3.2 Modeling with Diffusion Neutronics:

Linear Mechanics Equation: The linear elastic wave equation, Eq. 5, is discretized using second order, explicit centered time, centered space scheme. The discrete form (Singh, 2014) of the linear elastic wave equation is:

$$\frac{1}{c^2}\frac{u_i^{n+1}\Delta t^{n-\frac{1}{2}} - u_i^n(\Delta t^{n-\frac{1}{2}} + \Delta t^{n+\frac{1}{2}}) + u_i^{n-1}\Delta t^{n+\frac{1}{2}}}{\frac{1}{2}(\Delta t^{n-\frac{1}{2}} + \Delta t^{n+\frac{1}{2}})\Delta t^{n-\frac{1}{2}}\Delta t^{n+\frac{1}{2}}} = \frac{u_{i+1}^n \Delta x_{i+\frac{1}{2}}^n - u_i^n(\Delta x_{i-\frac{1}{2}}^n + \Delta x_{i+\frac{1}{2}}^n) + u_{i-1}^n \Delta x_{i+\frac{1}{2}}^n}{\frac{1}{2}(\Delta x_{i-\frac{1}{2}}^n + \Delta x_{i+\frac{1}{2}}^n)\Delta x_{i-\frac{1}{2}}^n \Delta x_{i+\frac{1}{2}}^n} - \frac{\alpha(1+\sigma)}{(1-\sigma)}\frac{T_{i+\frac{1}{2}}^n - T_{i-\frac{1}{2}}^n}{\Delta x_i^n}, \qquad (23)$$

where, n is the time step index. This second-order wave equation requires that we impose a set two initial conditions and two boundary conditions. There is a fixed surface condition on the left boundary, i.e. $u(0, t) = 0$, and a free surface condition on the right boundary, i.e. $\frac{\partial u}{\partial x}|_{x=L} = 0$. We use a Neumann boundary condition with $\frac{\partial u}{\partial t}|_{t=0} = 0$, and a Dirichlet boundary condition with $u(x, 0) = 0$.

Neutron Diffusion Equation: The transient diffusion equation, Eq. 3, is discretized using the finite volume method in space and implicit backward difference method in time. The discrete form of the transient neutron diffusion equation is

$$\frac{1}{\vartheta}\frac{\Phi^{n+1}_{i+\frac{1}{2}} - \Phi^{n}_{i+\frac{1}{2}}}{\Delta t^n}\Delta x_{i+\frac{1}{2}} - D_{i+1}\frac{\Phi^{n+1}_{i+\frac{3}{2}} - \Phi^{n+1}_{i+\frac{1}{2}}}{\Delta x_{i+1}} + D_{i-1}\frac{\Phi^{n+1}_{i+\frac{1}{2}} - \Phi^{n+1}_{i-\frac{1}{2}}}{\Delta x_{i-1}} + \Sigma^{n+1}_{a,i+\frac{1}{2}}\Phi^{n+1}_{i+\frac{1}{2}}\Delta x_{i+\frac{1}{2}} \tag{24}$$

$$= \upsilon\Sigma^{n+1}_{f,i+\frac{1}{2}}\Phi^{n+1}_{i+\frac{1}{2}}\Delta x_{i+\frac{1}{2}}.$$

There is a reflecting boundary condition on the left, i.e. $\frac{\partial \Phi}{\partial x} = 0|_{x=0}$ and a vacuum boundary condition on the right, i.e. $J^-(x = L) = 0$, where $J^-(x = L)$ is the incoming partial current at position L. To initialize neutronics, we run the eigenvalue problem. Then, we amplify the eigenflux such that the system power is approximately unity. This amplified flux is used as the initial flux.

Adiabatic heat-up: The temperature equation, Eq. 7, is discretized in time using the implicit backward difference formulation. The discretized form of the temperature equation is as follows:

$$\rho^{n+1}_{i+\frac{1}{2}}c_p \frac{T^{n+1}_{i+\frac{1}{2}} - T^{n}_{i+\frac{1}{2}}}{\Delta t^n} = \omega\Sigma^{n+1}_{f,i+\frac{1}{2}}\Phi^{n+1}_{i+\frac{1}{2}}. \tag{25}$$

Since there is no spatial derivative, boundary conditions are not required. To initialize the temperature, we set it to a uniform temperature field of 290K.

Simulation

We insert three different reactivities into a critical FBR system to observe the material response. This reactivity insertion leads to temperature increase due to increased fission. Subsequently, mechanical feedback reduces the density and macroscopic cross sections which leads the reactor to shut down. Due to lack of heat loss mechanism in our model, the system stays in an expanded

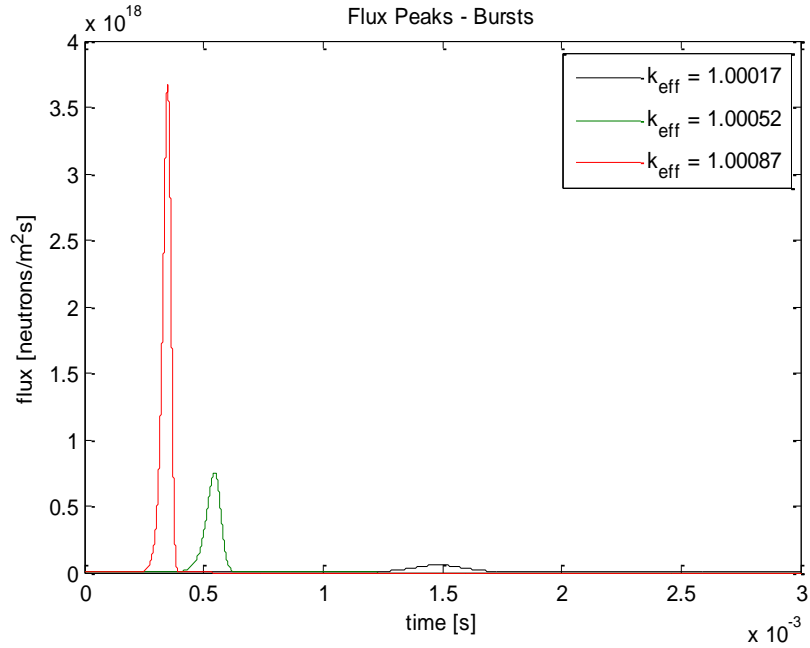equilibrium state. Figures 5a, 5b, and 5c demonstrate system's material response to the three reactivity insertions.

Figure 5a: System's material response – flux peaks
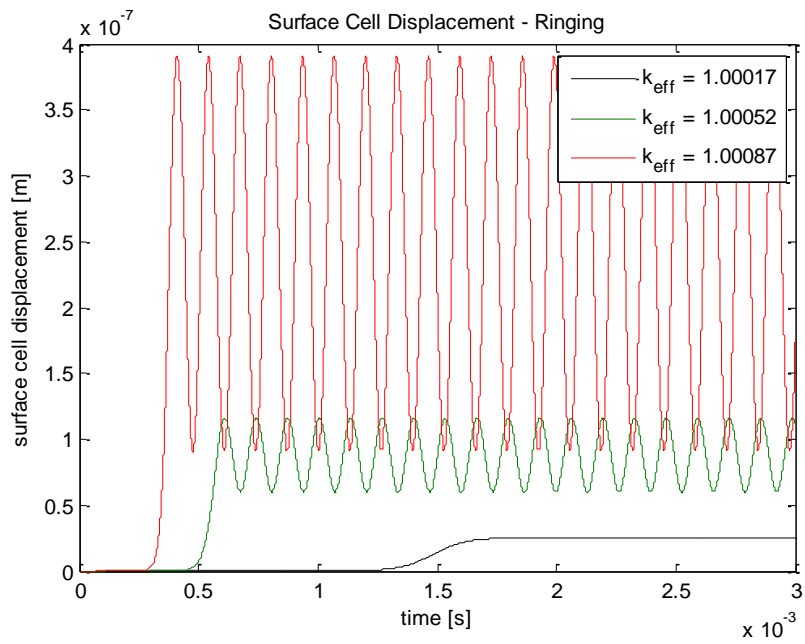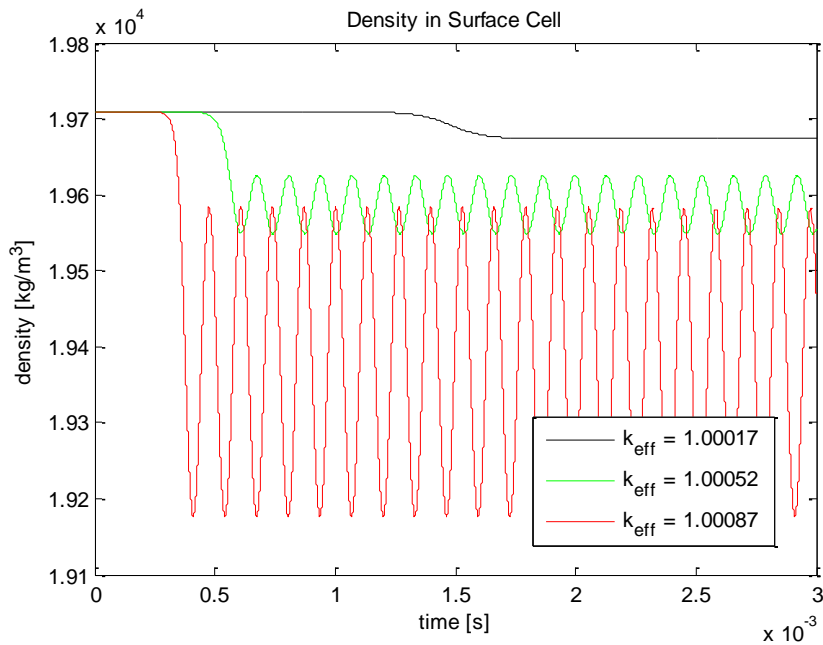

Figure 5b: System's material response – displacements

Figure 5c: System's density response

Note that a low enough reactivity insertion follows exactly what is expected – the system expands and stays in that expanded equilibrium state. If, however, the reactivity insertion is high enough, we observe the ringing effect – periodic oscillation of displacements. This vibrational effect is attributed to the fact that, for higher reactivity insertion, the power increases too fast for the material to respond in time. Please refer to (Kadioglu et al., 2009) for numerical analysis where it is claimed that of the ratio squared of linear mechanics time scale and neutronics time scale is too small, time derivative on the non-dimensional wave equation becomes insignificant. Thus that equation stops supporting wave structure in the solution of material response. In all other cases where the time derivative is significant, wave structure is supported and vibrations are observed.

The goal of this study is to extend the IMEX algorithm to incorporate transport effects. In the following subsections, we will demonstrate why transport neutronics is desired and discuss the difference between system's material response to diffusion and transport neutronics.

22

3.3 Extension to Transport Neutronics

Why Extend to Transport Neutronics

To demonstrate the importance of transport neutronics, we present the difference between the flux from diffusion and transport eigenvalue calculations for the present FBR system. The system is small so we see noticeable transport effects on the flux (Figure 6) and flux gradient. Since the temperature is directly proportional to the fission rate and the forcing term on the elastic wave equation is proportional to the temperature gradient, we expect the overall solution of the coupled system with transport neutronics to differ from that with diffusion neutronics.
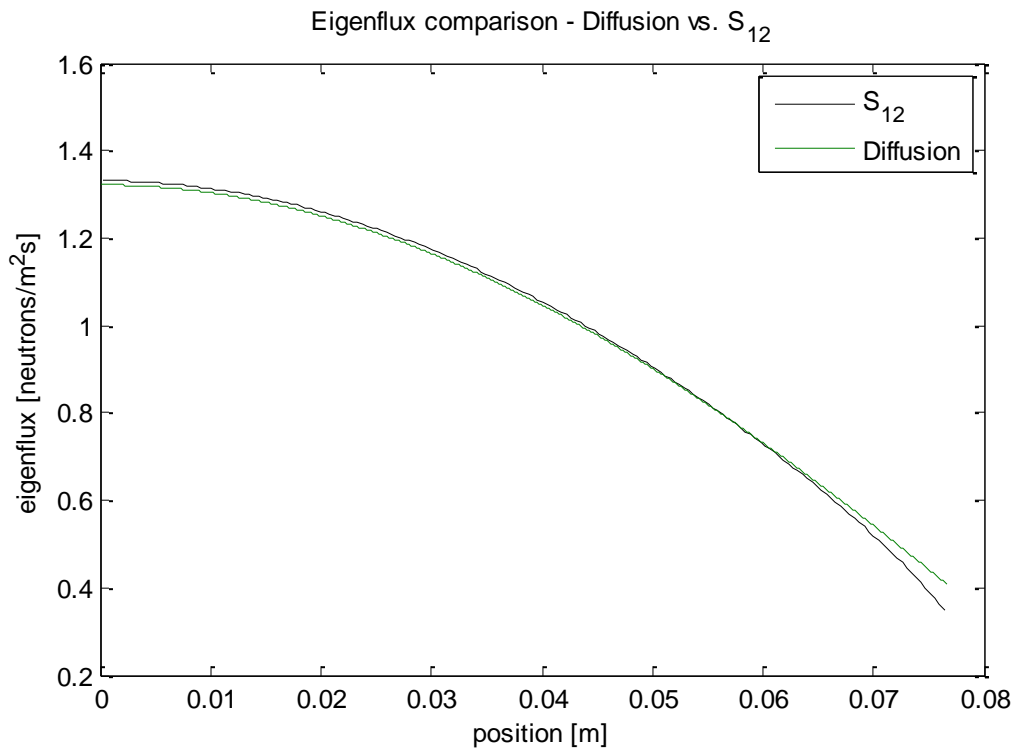

Figure 6: Eigenflux vs. position – Diffusion & Transport (S_{12})

This difference in the two neutronics models motivates us to extend the IMEX algorithm presented in (Kadioglu et al., 2009) to incorporate transport effects. This is done using the transport equation to model neutronics.

Discretization

The transient transport equation, Eq. 2, is discretized in space using diamond difference, and in angle using the S_N method. We use the one group approximation for treatment of energy, and we assume isotropic scattering. We use Backward Euler (BDF-1) implicit time stepping. The following equation represents the time discrete form of the transport equation:

$$\frac{1}{\vartheta}\frac{\psi_{i+\frac{1}{2},m}^{n+1,g}-\psi_{i+\frac{1}{2},m}^{n,g}}{\Delta t^n} + \mu_m\frac{\psi_{i+1,m}^{n+1,g}-\psi_{i,m}^{n+1,g}}{\Delta x_{i+\frac{1}{2}}} + \Sigma_{t,i+\frac{1}{2}}^{n+1}\psi_{i+\frac{1}{2},m}^{n+1,g} = \frac{1}{2}(\Sigma_{s,i+\frac{1}{2}}^{n+1} + v\Sigma_{f,i+\frac{1}{2}}^{n+1})\Phi_{i+\frac{1}{2}}^{n+1,g-1}. \tag{26}$$

Here, m is the angular cosine index, g is the iteration index, and μ_m is the mth angular cosine.

We have the same discrete forms of the wave equation and temperature equation as given by Eq. 23 and Eq. 25 respectively.

Coupling Scheme

In order to incorporate transport neutronics in our FBR model, we simply replace the diffusion equation by the transport equation. As a result, we have the following Newton system:

$$\begin{pmatrix} \mathbb{J}_{uu} & 0 & 0 \\ \mathbb{J}_{\psi u} & \mathbb{J}_{\psi\psi} & 0 \\ \mathbb{J}_{Tu} & \mathbb{J}_{T\psi} & \mathbb{J}_{TT} \end{pmatrix}\begin{bmatrix} \delta u \\ \delta\psi \\ \delta T \end{bmatrix} = -\begin{bmatrix} F_u \\ F_\psi \\ F_T \end{bmatrix}, \tag{27}$$

where, the residual function, F_ψ, is as follows:

$$F_\psi = \frac{1}{\vartheta}\frac{\partial\psi}{\partial t} + \mu\frac{\partial\psi}{\partial x} + \Sigma_t\psi - \frac{1}{2}(\Sigma_s + v\Sigma_f)\,\Phi. \tag{28}$$

Note that the system of Eq. 27 is still one-way coupled in physics, so we can solve it in a sequential way.

Simulation

Again, we insert different reactivities and observe the material response. Here, we insert two different reactivities with k_{eff} of 1.00017 and 1.000095 to observe the system response. Just like with diffusion, we expect the system to go to a steady expanded state with adequately low reactivity insertion, and ring with high enough reactivity insertion.
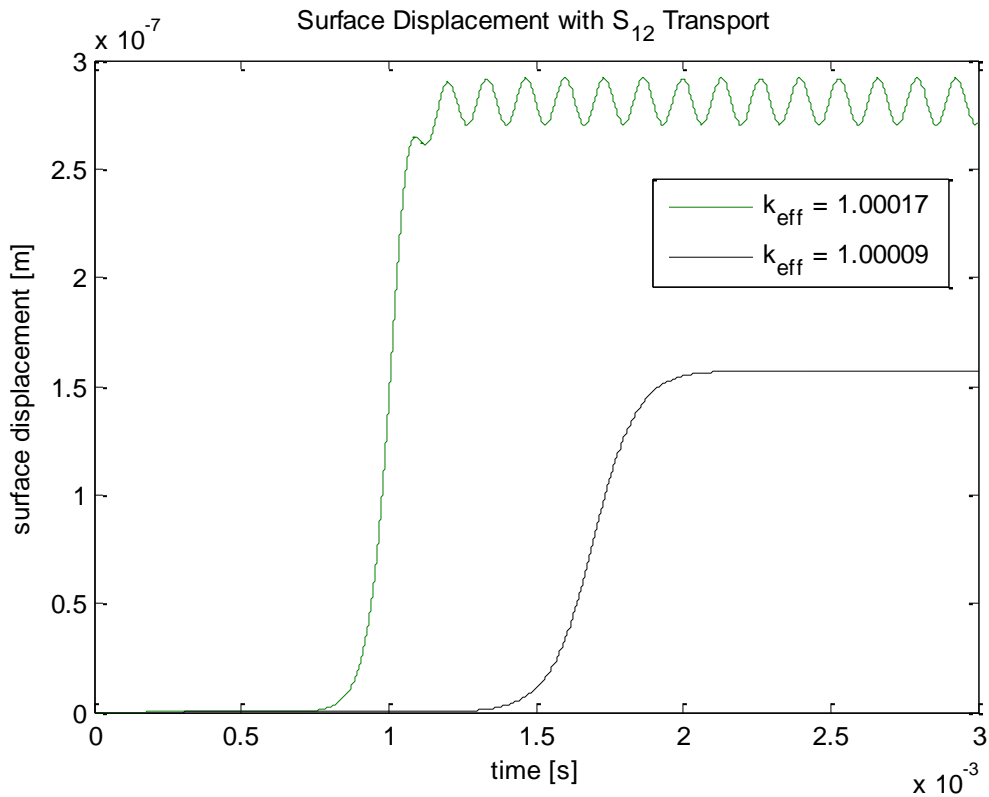

Figure 7: Surface cell displacement with transport neutronics for varying reactivity insertion.

From Figure 7, we observe that different reactivity insertions lead to different equilibrium states. The system expands and stays in that expanded state for low reactivity insertion due to lack of heat removal mechanism in our model. At the same time, with high enough reactivity insertion, we observe the ringing effect. This phenomenon may again be attributed to the difference in dynamical time scales between neutronics and linear mechanics.

25

In conclusion, we observe similar material behavior with transport as we observed with diffusion. However, note the difference in k_{eff} used for transport and diffusion. This is a major discrepancy. In the next subsection, we will present a detailed comparison between diffusion and transport models with respect to FBR transient simulations.

Comparison of Material Response – Diffusion vs. Transport Neutronics

We observed, earlier in this section, that the eigenflux resulting from diffusion and transport calculations for this system had different shapes. The effects of this difference in flux, and flux gradient will be seen in this subsection. First, we present how the material response of low reactivity insertion to diffusion and transport neutronics differ.
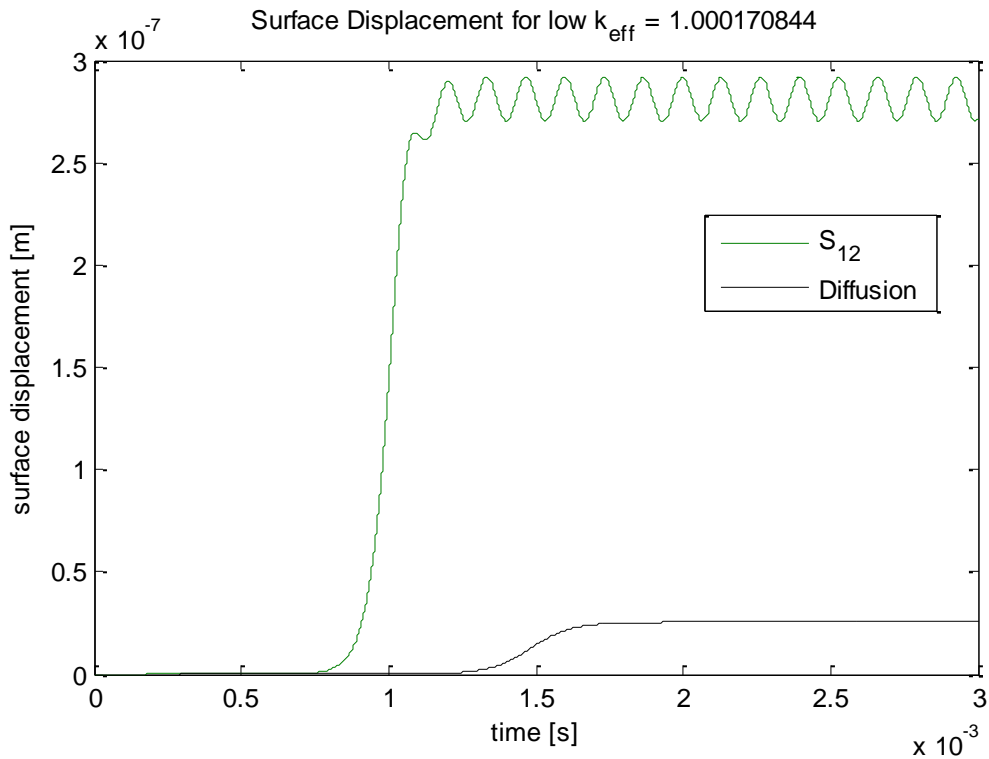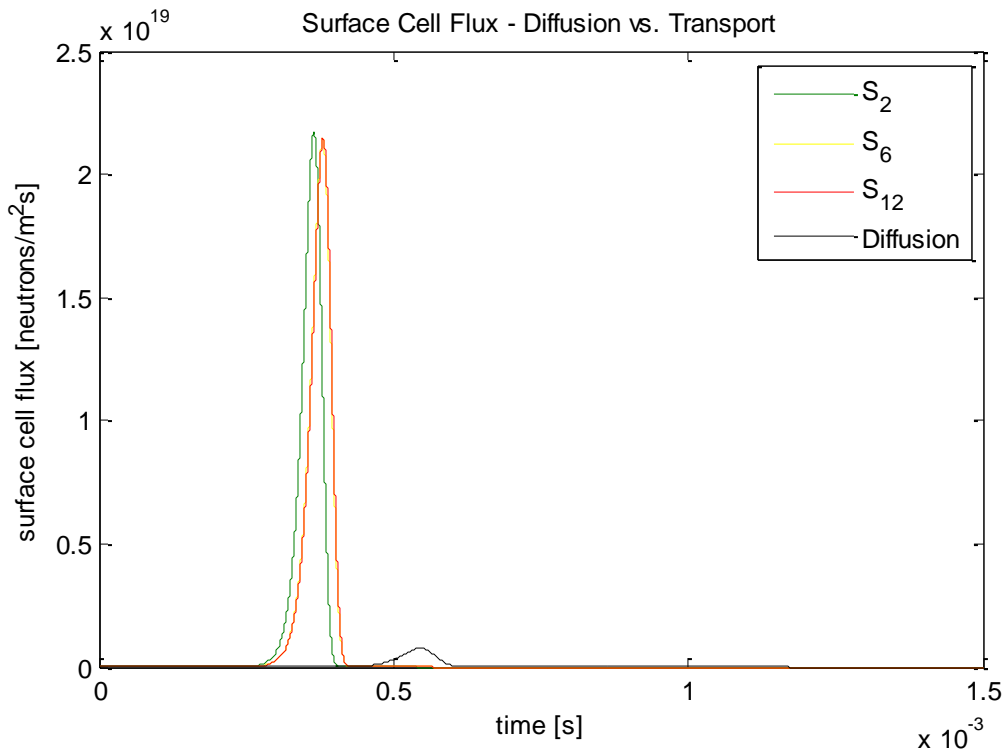

Figure 8: Surface cell displacement evolution with time – Diffusion vs. Transport (S_{12})

From Figure 8, we observe that for a small reactivity insertion, with k_{eff} of 1.00017, the system rings with transport neutronics but the system goes to an expanded non vibrational state with diffusion neutronics. This results from the difference in the dynamical time scales that diffusion and transport neutronics exhibit. We note that flux evolution of the system with diffusion neutronics is slow enough for the system to settle into a new equilibrium state after undergoing material expansion. That, however, is not the case with transport neutronics where the material response doesn't keep up with the flux evolution in time. Therefore, we observe material ringing with transport neutronics for this particular reactivity insertion.

Then we do the same kind of analysis for a slightly higher k_{eff} of 1.00052. We look at the difference in the material response to different neutronics models.

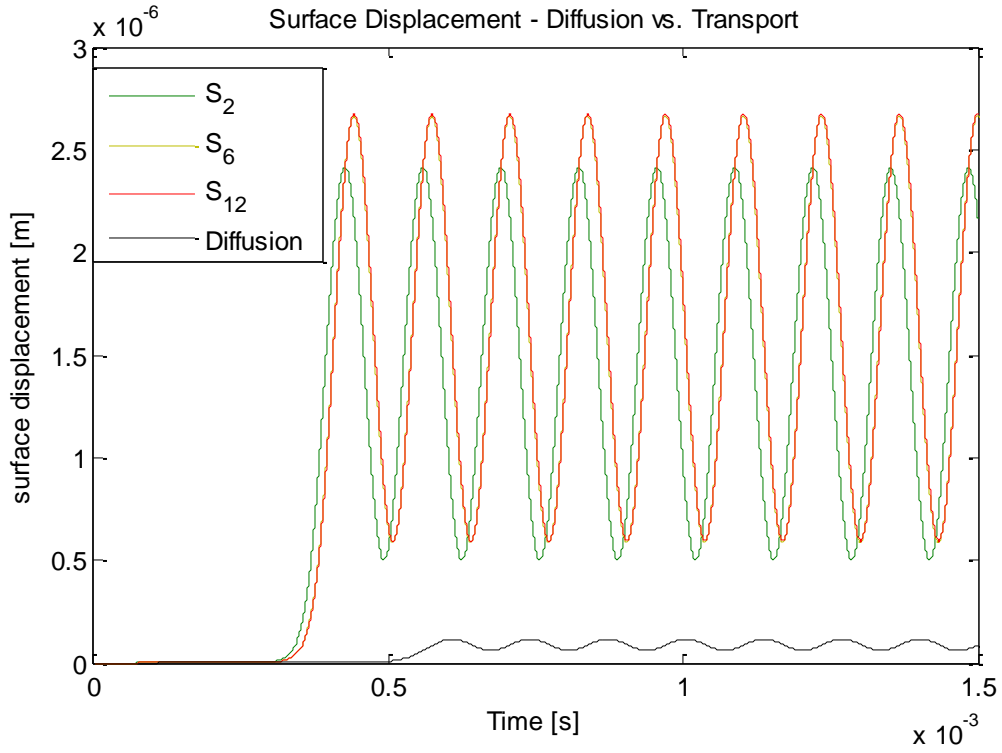**Figure 9: Flux peaks with different neutronics approximations**

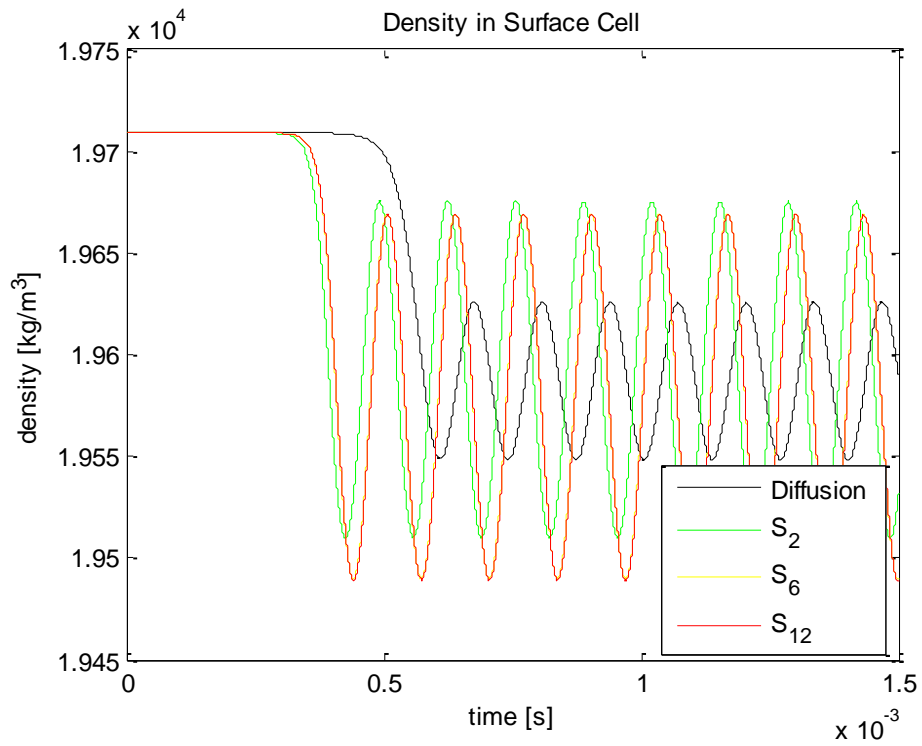**Figure 10a: Surface cell displacements with different neutronics approximations**

Figure 10b: Surface cell density with different neutronics approximations

28

We see different amplitudes and phases in surface oscillations with different neutronics models. To understand this we go back to the comparison of eigenflux in Figure 6. We see how different neutronics models produce different flux profiles, and therefore different flux gradients. The temperature depends directly on the flux, and the temperature gradient forms the forcing term for the wave equation. Thus different flux profiles result in different forcing terms on the wave equation which cause the material response to be different with different neutronics models.

In particular, note the difference between the material response to diffusion and S_2 transport. While we expect diffusion to be equivalent to S_2 in steady state, they differ in transient settings. We observe that here. The reason for this difference between results from diffusion, and S_2 neutronics is that the diffusion equation is parabolic, while the S_2 equation is hyperbolic. The two have different properties which translate into different system behavior.

Other than that, we see that different angular resolution on transport results in different material behavior also (Figures 9, 10a, and 10b). This may again be traced back to different forcing term on the wave equation. We must note that once optimal angular resolution is reached, improvement in angular resolution has minimal effect on the material response of the system, as seen in the case of Figures 9 and 10a. That is again expected since converged flux profile that results from optimal angular resolution does not change much further with increasing angular resolution which means that the forcing terms do not change much either. This results in converging material response with increasing angular resolution. We observe that as we go from S_2 to S_6 and finally to S_{12}.

Another reason one may observe this difference between material responses from different neutronics models is that the time scales on each model may be different. Figure 9 suggests that the flux pulse build up times are significantly different between for the different neutronics models. This means that the neutron multiplication time scale is longer for diffusion model as compared to

the transport model. This is expected since the diffusion model exhibits more neutron leakage and higher scattering.

Now, we note that source iteration is not necessarily the best way to solve the transport equation. We also note the benefit in isolating the angular flux from the coupled system, especially while we are dealing with a more complicated 3D system or a fully coupled nonlinear system, while retaining the transport effects. This can be done by introducing the moment based acceleration – scale bridging HOLO concept – into the neutronics model. We will discuss this concept in the next section.

Chapter 4: Extension to Moment Based Acceleration

In this section, we extend the IMEX scheme to incorporate moment-based acceleration (Smith et al., 2002), (Knoll et al., 2011), (Park et al., 2012) for neutronics into the coupled system. One of its main advantages, as the name suggests, is that it accelerates slowly converging physics like fission and/or scattering source. This reduces the number of iterations required per time-step to get the new scalar flux. This fact is widely known. The other advantage is that it allows us to isolate the angular flux from the coupled system by introducing a discretely consistent LO system which resembles the diffusion equation. This moment based acceleration concept is a scale bridging concept because it essentially bridges transport and diffusion equations with distinct corresponding length scales using the drift term in the LO equation.

4.1 Standard S_N vs. Nonlinear Diffusion Accelerated S_N (Moment-Based Acceleration)

Here, we show consistency of the accelerated transport solution to the eigenvalue problem for the present fast burst system. The problem parameters have been stated in section 4.1. Figure 11 shows a comparison between the standard S_N solution and the accelerated S_N solution. We observe that the nonlinear diffusion accelerated S_N follows the standard S_N solution quite closely. The relative error norm was found to be 1.7043×10^{-9}.

The total number of transport sweeps required with standard S_N was 156, while the total number required with HOLO (NDA S_N) iteration was 19. Clearly, if we were to solve a transient coupled problem, which could involve several hundred thousand time-steps, then using accelerated S_N instead of standard S_N with source iteration would be a good idea. Therefore this is one reason why we proceed to extend the present IMEX algorithm to incorporate moment-based acceleration concept. The other reason will be explained in the next subsection.
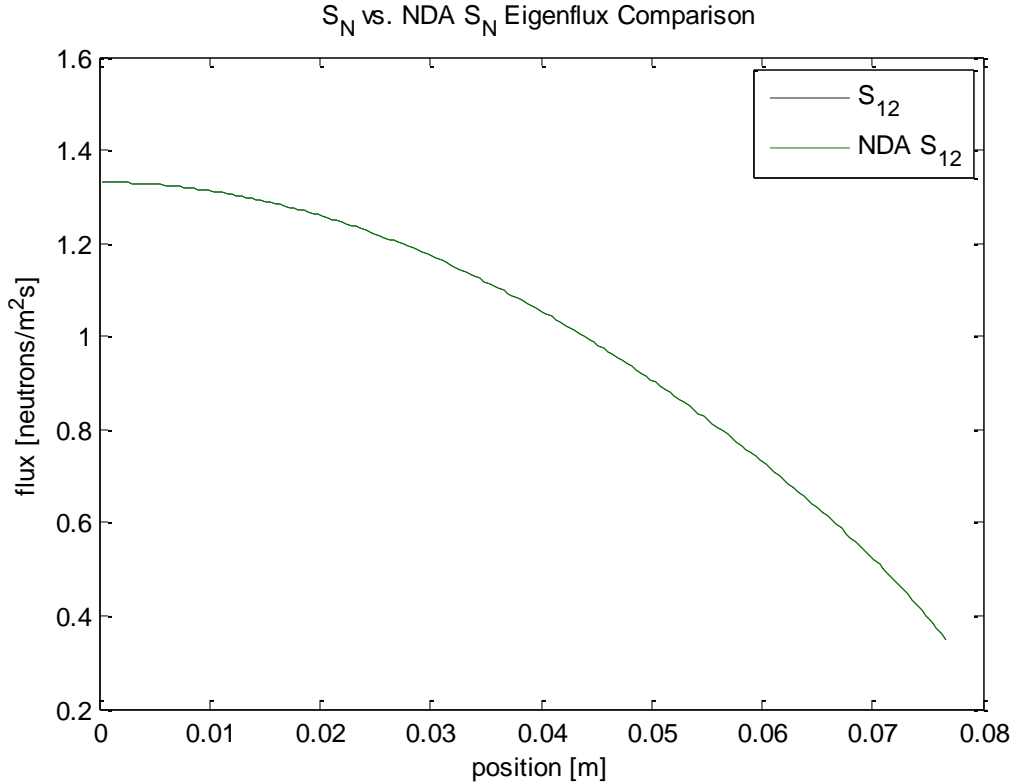
Figure 11: Eigenflux comparison for the fast burst reactor problem

4.2 Moment-Based Acceleration – Concept, Equations and Discretization

The transport equation can have a large dimensions (up to 7D) so we want to isolate the transport solver from the coupled system. By introducing a "discretely consistent" lower-order (LO) system we can separate out the expensive transport solver from the coupled system (Knoll et al., 2011).

The basic idea behind moment based acceleration technique is the reduction of complicated higher order (HO) equation, by taking a moment, into a lower order (LO) equation with fewer degrees of freedom. In other words, we integrate out a dependency from the HO equation to get the LO equation. The LO equation is equivalent to the HO equation. This transformation of the HO system into the LO system has the potential to be very useful in multiphysics simulations since the LO

32

equation has lower dimensions. Consider a tightly coupled nonlinear problem where iteration between physics is necessary. It is advantageous to minimize the dimensions for such nonlinear problems. This is where the moment based acceleration concept becomes very useful since it allows us to substitute the large dimensional HO system by a lower dimensional LO system while preserving essential physics represented by the HO system. In the case of the FBR problem, we want to isolate the transport solver from the coupled system while preserving transport effects. This can be done by introduction of moment based acceleration into the transport solver.

Now, we want to apply moment-based acceleration technique to the transport solver. Therefore the transport equation, Eq. 2, becomes our HO system. The next step is to integrate out the angular dependency. We take the zeroth angular moment of the transport equation to obtain Eq. 1, which forms the LO system. Now, Eq. 1 comes with a new variable – current J for which we provide the standard diffusion plus drift closure. Therefore, the equation system can be written as,

Higher Order (HO) system:

$$\frac{1}{\vartheta}\frac{\partial \psi}{\partial t} + \mu\frac{\partial \psi}{\partial x} + \Sigma_t \psi = \frac{1}{2}\left(\Sigma_s + \nu\Sigma_f\right)\Phi^{LO}, \tag{29}$$

Lower Order (LO) system:

$$\frac{1}{\vartheta}\frac{\partial \Phi^{LO}}{\partial t} + \frac{\partial J}{\partial x} + \Sigma_a \Phi^{LO} = \nu\Sigma_f \Phi^{LO}, \tag{30}$$

Closure:

$$J = -D\frac{\partial \Phi^{LO}}{\partial x} + \widehat{D}\Phi^{LO} \tag{31}$$

where,

$$\widehat{D} = \frac{J^{HO} + D\frac{\partial \Phi^{HO}}{\partial x}}{\Phi^{HO}}, \qquad J^{HO} = \int_{-1}^{1} \mu\psi d\mu \qquad (32)$$

To make sure our HO, and LO systems are consistent, and for acceleration, we make the drift coefficient, $\widehat{D}$, a function of angular flux from the HO system (Knoll et al., 2011). This makes the system nonlinear. Thus, solving it with Picard iteration, first, a transport sweep is carried out for calculation of HO angular and HO scalar flux. Then, with this set of new angular fluxes, new drift coefficients are calculated which, in turn, are used to solve the LO system. We iterate until the HO and the LO scalar fluxes converged to the given tolerance.

For clarity, we provide the discretized forms of the relevant equations in order in which they are solved to achieve moment based acceleration. We start with a transport sweep. We discretize the HO system using diamond difference in space and discrete ordinates in angle. We use BDF-1, and BDF-2 schemes for time discretization. We use BDF-1 time stepping for testing the accuracy of HOLO algorithm since we test it against standard S_N transport solution with BDF-1 time stepping. In order to investigate the order of accuracy of the algorithm, we use BDF-2 time stepping. The discrete forms of the HO equation with BDF-1 and BDF-2 time discretization are respectively,

$$\frac{1}{\vartheta}\frac{\psi_{i+\frac{1}{2},m}^{n+1,g} - \psi_{i+\frac{1}{2},m}^{n}}{\Delta t^n} + \mu_m \frac{\psi_{i+1,m}^{n+1,g} - \psi_{i,m}^{n+1,g}}{\Delta x_{i+\frac{1}{2}}} + \Sigma_{t,i+\frac{1}{2}}^{n+1}\psi_{i+\frac{1}{2},m}^{n+1,g} = \frac{1}{2}(\Sigma_{s,i+\frac{1}{2}}^{n+1} + \nu\Sigma_{f,i+\frac{1}{2}}^{n+1})\Phi_{i+\frac{1}{2}}^{LO,n+1,g-1}, \qquad (33)$$

$$\frac{1}{\vartheta}\frac{\frac{3}{2}\psi_{i+\frac{1}{2},m}^{n+1,g} - 2\psi_{i+\frac{1}{2},m}^{n} + \frac{1}{2}\psi_{i+\frac{1}{2},m}^{n-1}}{\Delta t^n} + \mu_m \frac{\psi_{i+1,m}^{n+1,g} - \psi_{i,m}^{n+1,g}}{\Delta x_{i+\frac{1}{2}}} + \Sigma_{t,i+\frac{1}{2}}^{n+1}\psi_{i+\frac{1}{2},m}^{n+1,g} = \frac{1}{2}(\Sigma_{s,i+\frac{1}{2}}^{n+1} + \nu\Sigma_{f,i+\frac{1}{2}}^{n+1})\Phi_{i+\frac{1}{2}}^{LO,n+1,g-1}. \qquad (34)$$

Here, the HO transport sweep solves for $\psi^{n+1,g}$ with given scattering and fission source, $\Phi^{LO,g-1}$.

Then, we calculate the drift coefficients at cell faces using the following discrete closure equation:

$$J_i^{HO,g} = -D_i^{n+1} \frac{\Phi_{i+\frac{1}{2}}^{HO,g} - \Phi_{i-\frac{1}{2}}^{HO,g}}{\Delta x_i} + \frac{\widehat{D}_i^g}{2}(\Phi_{i+\frac{1}{2}}^{HO,g} + \Phi_{i-\frac{1}{2}}^{HO,g}) \tag{35}$$

where,

$$J_i^{HO,g} = \int_{-1}^{1} \mu \psi_i^g \, d\mu. \tag{36}$$

After calculating the drift coefficients, we solve the LO system. We discretize the LO system using finite difference method for discrete consistency with the HO system. Again, we use implicit BDF-1 and BDF-2 for time discretization. We calculate the new LO scalar fluxes respectively using the following BDF-1 and BDF-2 discrete equations:

$$\frac{1}{\vartheta} \frac{\Phi_{i+\frac{1}{2}}^{\star,LO} - \Phi_{i+\frac{1}{2}}^{n,LO}}{\Delta t^n} + \frac{J_{i+1}^{\star,LO} - J_i^{\star,LO}}{\Delta x_{i+\frac{1}{2}}} + \Sigma_{a,i+\frac{1}{2}}^{n+1} \Phi_{i+\frac{1}{2}}^{\star,LO} = \nu \Sigma_{f,i+\frac{1}{2}}^{n+1} \Phi_{i+\frac{1}{2}}^{\star,LO}, \tag{37}$$

$$\frac{1}{\vartheta} \frac{\frac{1}{2}\Phi_{i+\frac{1}{2}}^{\star,LO} - 2\Phi_{i+\frac{1}{2}}^{n,LO} + \frac{1}{2}\Phi_{i+\frac{1}{2}}^{n-1,LO}}{\Delta t^n} + \frac{J_{i+1}^{\star,LO} - J_i^{\star,LO}}{\Delta x_{i+\frac{1}{2}}} + \Sigma_{a,i+\frac{1}{2}}^{n+1} \Phi_{i+\frac{1}{2}}^{\star,LO} = \nu \Sigma_{f,i+\frac{1}{2}}^{n+1} \Phi_{i+\frac{1}{2}}^{\star,LO}, \tag{38}$$

where,

$$J_i^{\star,LO} = -D_i^{n+1} \frac{\Phi_{i+\frac{1}{2}}^{\star,LO} - \Phi_{i-\frac{1}{2}}^{\star,LO}}{\Delta x_i} + \frac{\widehat{D}_i^g}{2}(\Phi_{i+\frac{1}{2}}^{\star,LO} + \Phi_{i-\frac{1}{2}}^{\star,LO}). \tag{39}$$

Here, the superscript $\star$ indicates time step n+1 and HOLO iteration index g. We solve the LO equation to get $\Phi^{\star,LO}$ while treating fission and scattering implicitly.

The most important attribute of the moment based acceleration concept, for the purpose of this work, is that HO and LO scalar fluxes are equivalent as that is built into the convergence criteria (i.e. $\Phi_{i+\frac{1}{2}}^{LO} = \Phi_{i+\frac{1}{2}}^{HO}$). Therefore, while solving a coupled multiphysics problem, it is valid to swap out the

angular flux dependent transport (equivalent to purely HO system) solver for the diffusion equation like diffusion plus drift LO system without affecting the solution of the problem (as long as the transport problem is solved within the HOLO framework).

4.3 Coupling Scheme

Next, we incorporate the moment based acceleration method into our IMEX algorithm. We begin by replacing the transport equation, in Eq. 27, with the LO equation. We get the following Newton step:

$$\begin{pmatrix} \mathbb{J}_{uu} & 0 & 0 \\ \mathbb{J}_{\Phi^{LO}u} & \mathbb{J}_{\Phi^{LO}\Phi^{LO}} & 0 \\ \mathbb{J}_{Tu} & \mathbb{J}_{T\Phi^{LO}} & \mathbb{J}_{TT} \end{pmatrix} \begin{bmatrix} \delta u \\ \delta\Phi^{LO} \\ \delta T \end{bmatrix} = -\begin{bmatrix} F_u \\ F_{\Phi^{LO}} \\ F_T \end{bmatrix}. \tag{40}$$

The residual function $F_{\Phi^{LO}}$ is given by,

$$F_{\Phi^{LO}} = \frac{1}{\vartheta}\frac{\partial \Phi^{LO}}{\partial t} - \frac{\partial}{\partial x}\left(D\frac{\partial \Phi^{LO}}{\partial x} + \widehat{D}\Phi^{LO}\right) + \Sigma_a\Phi^{LO} - \upsilon\Sigma_f\Phi^{LO}. \tag{41}$$

Note that we still have a one way coupled system which may be solved sequentially.

One may not necessarily see merit in replacing the angular flux for LO scalar flux in this particular problem because of the one way coupling – we could couple the HO transport equation directly for the multiphysics system (not isolating the angular variable) and the problem would still essentially stay the same as long as we did our neutronics using a moment based acceleration technique. But imagine a two way coupled problem, as stated before, where iteration between physics is necessary - that is where this kind of substitution of equations can be really useful.

Another advantage of using the LO flux in the coupled system is the ease with which we can transition from diffusion to transport as the LO system resembles the diffusion equation. All we

need to do is add a consistency term to the existing diffusion solver (plus a transport sweep for calculation of the consistency term - outside the coupled system).

4.4 Simulation

In this section, we demonstrate how the introduction of moment based acceleration to the neutronics affects the material response of the coupled system. We consider a test problem with k_{eff} of 1.00052 and compare the material response, in time, of the coupled systems with standard S_N – represented by Eq. 27 and HOLO S_N – represented by Eq. 40. Material parameters, for this problem, have been presented in section 3. Figures 12a and 13a present a comparison between surface cell displacements and fluxes from the two neutronics models. Note that surface flux and displacement profiles from the two models follow each other quite well. The relative errors, between the L_2 norms, in the surface cell displacement, and surface cell flux were found to be 3.15×10^{-4}, and 7.01×10^{-4} respectively.

We also present plots of the relative error in the L_2 norm of the spatial displacement (Figure 12b) and neutron flux (Figure 13b) at every time-step in order to examine the differences between the two models. In Figure 12b, we note a spike in the relative error in L_2 norm of displacement at time 5.182×10^{-5} s where the value of the norm is practically 0 (of the order of 10^{-22}). This spike is an artifact of round off errors. At all times, we see low relative error which is acceptable. We also note the periodic nature to the error once the system starts ringing. Similarly in figure 13b, with neutron flux, we note acceptable relative error in L_2 norm values. We also note oscillations, and an increasing error trend as the flux magnitude diminishes to insignificant values.
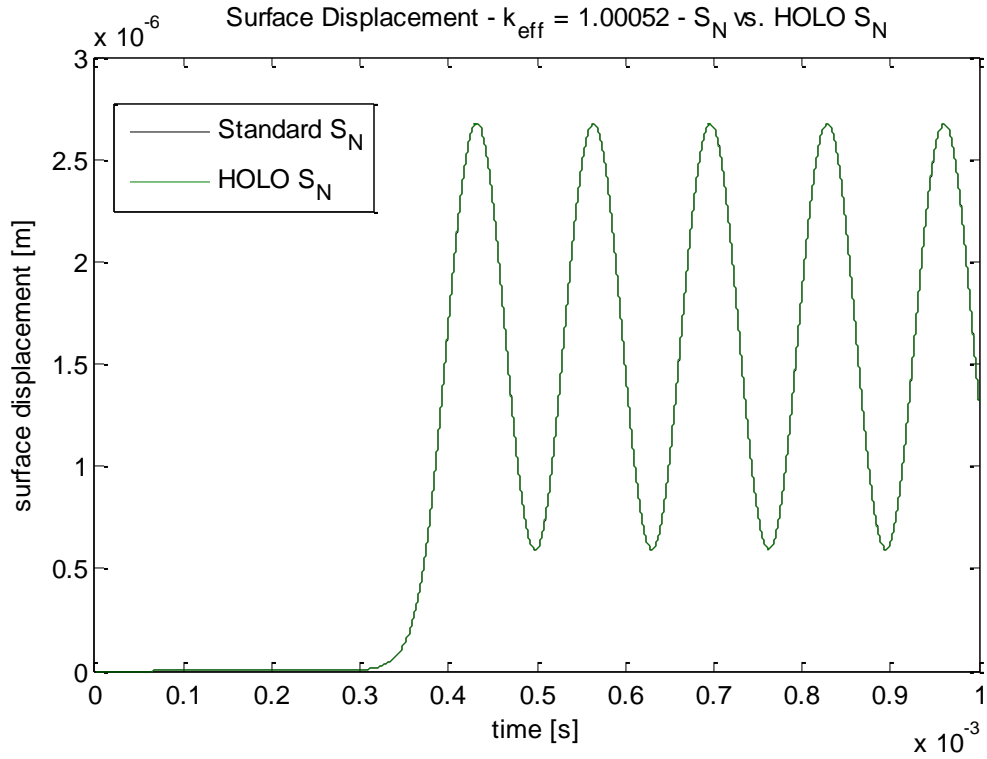
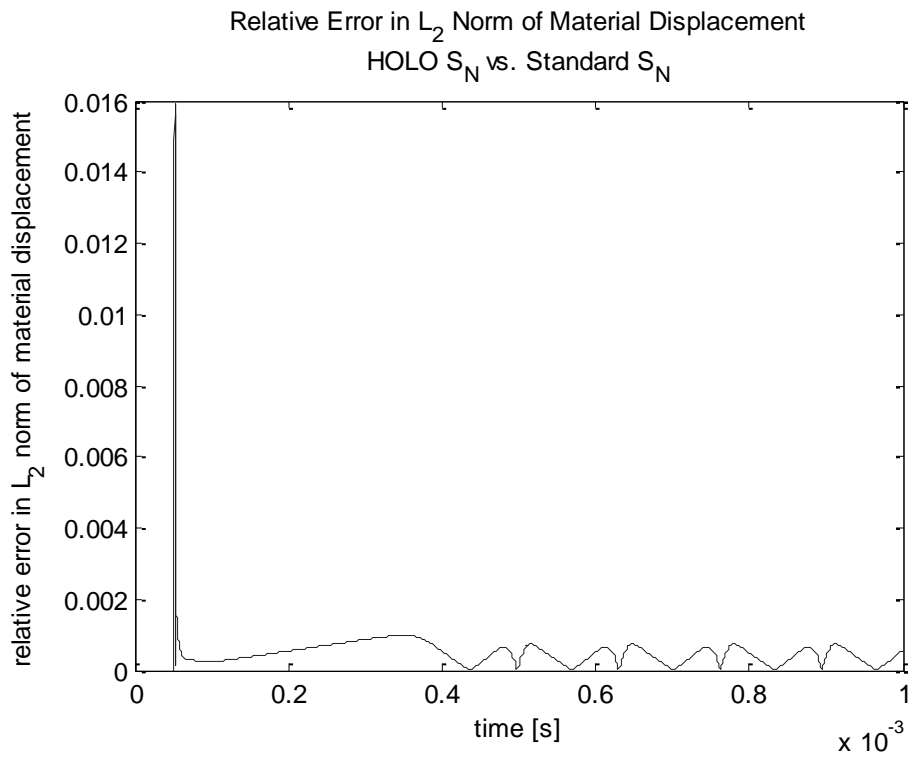**Figure 12a: Surface displacements – HOLO (NDA) S$_N$ vs. Standard S$_N$**

Figure 12b: Relative error in the L$_2$ norm of the spatial displacement at each time step – HOLO (NDA) S$_N$ vs. Standard S$_N$
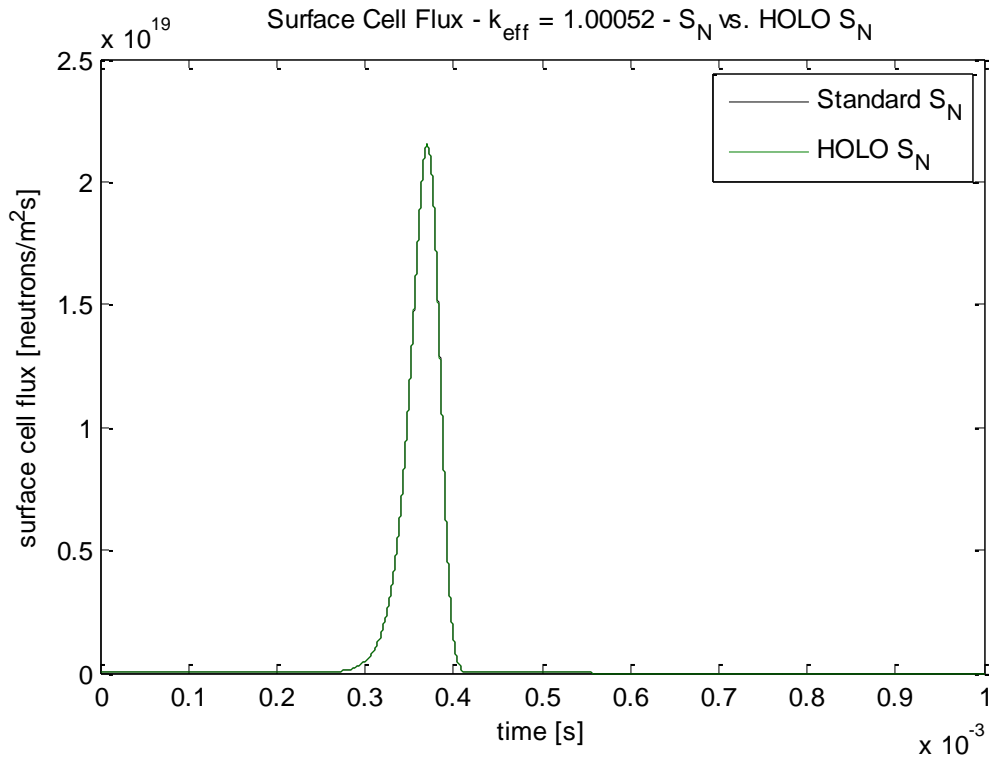
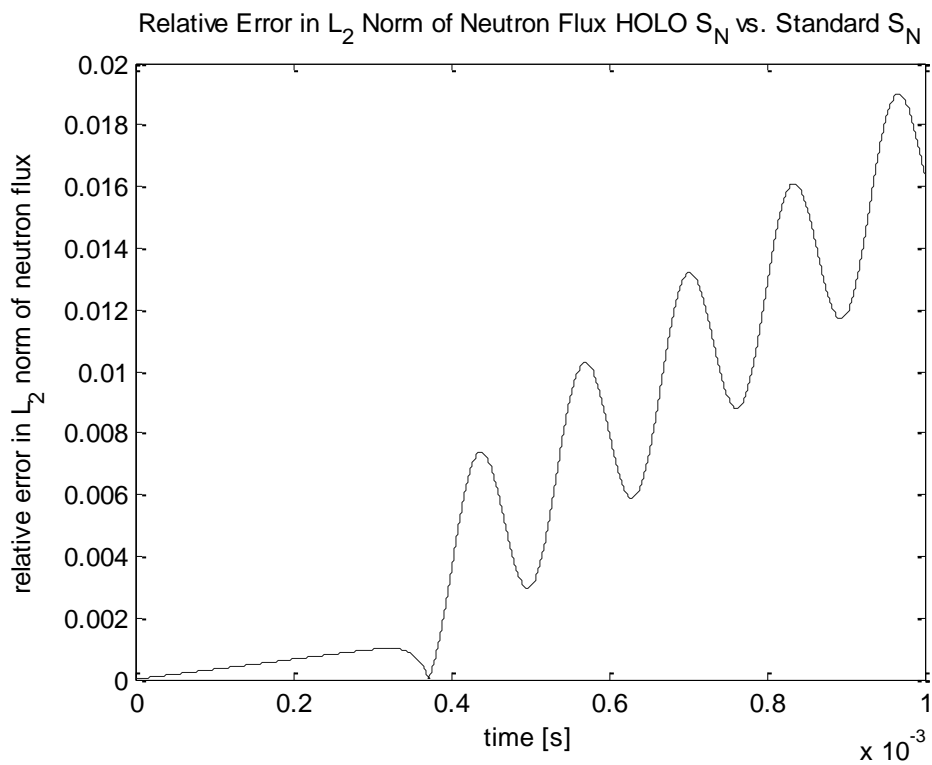**Figure 13a: Surface fluxes – HOLO (NDA) S_N vs. Standard S_N**

Figure 13b: Relative error in the L₂ norm of the neutron flux at each time step – HOLO (NDA) S_N vs. Standard S_N

The plots examined in this subsection, along with satisfactory error norm numbers, prove the applicability of the HOLO concept in true (although simplified) multiphysics setting.

4.5 Convergence Study

Now, we look at the convergence rate for scalar flux, material displacement in order to determine the quality of the coupled solution with HOLO transport neutronics, and IMEX coupling. To do that, we use implicit BDF-2 time integration scheme for neutronics, and the temperature equations. Then we run the transient coupled problem with five distinct time steps ranging from 1×10^{-7} to 6.25×10^{-9} s, for 0.5 ms time. We choose the total number of time steps, accordingly, for each time step size. Table 1, along with figure 14 and figure 15, presents the data collected after running the five transient simulations for this convergence study.

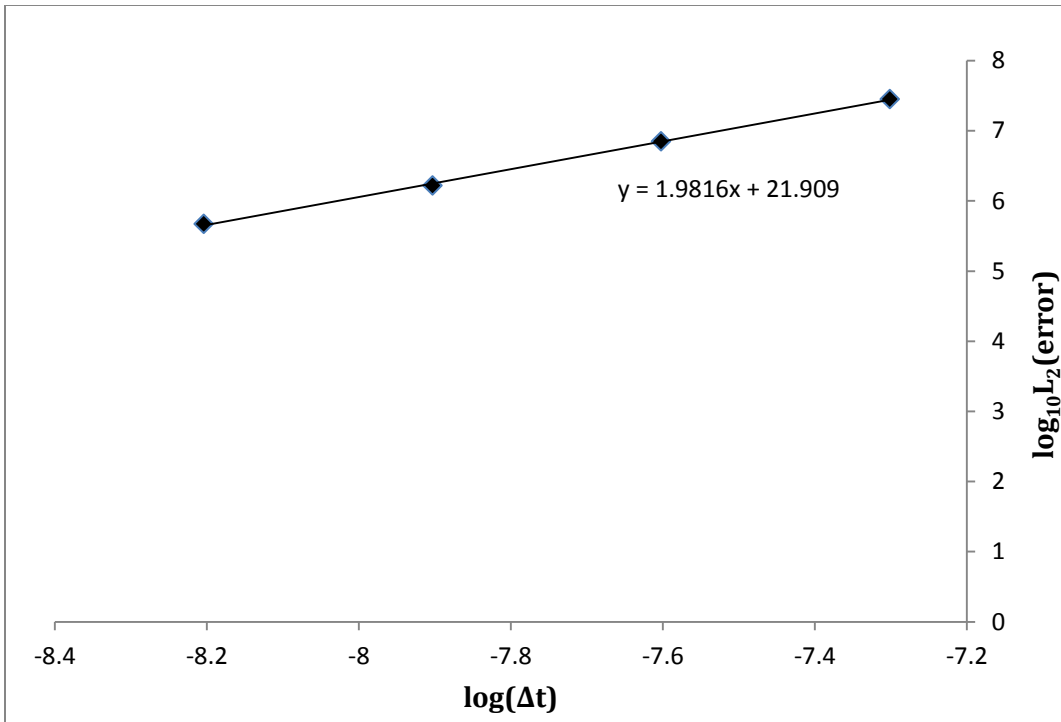| Time step (Δt)	Log(Δt)	Log($\|$flux(Δt) – flux($\Delta t/2$)$\|$)	Log($\|$u(Δt) – u($\Delta t/2$)$\|$)
5×10^{-8}	-7.301029995663981	7.447863755282549	-9.641079015622641
2.5×10^{-8}	-7.602059991327963	6.847704077101912	-10.189050265316403
1.25×10^{-8}	-7.903089986991944	6.217734674605953	-11.088037041790605
6.25×10^{-9}	-8.204119982655925	5.669407487493253	-11.162963763319620

Table 1: Convergence Data

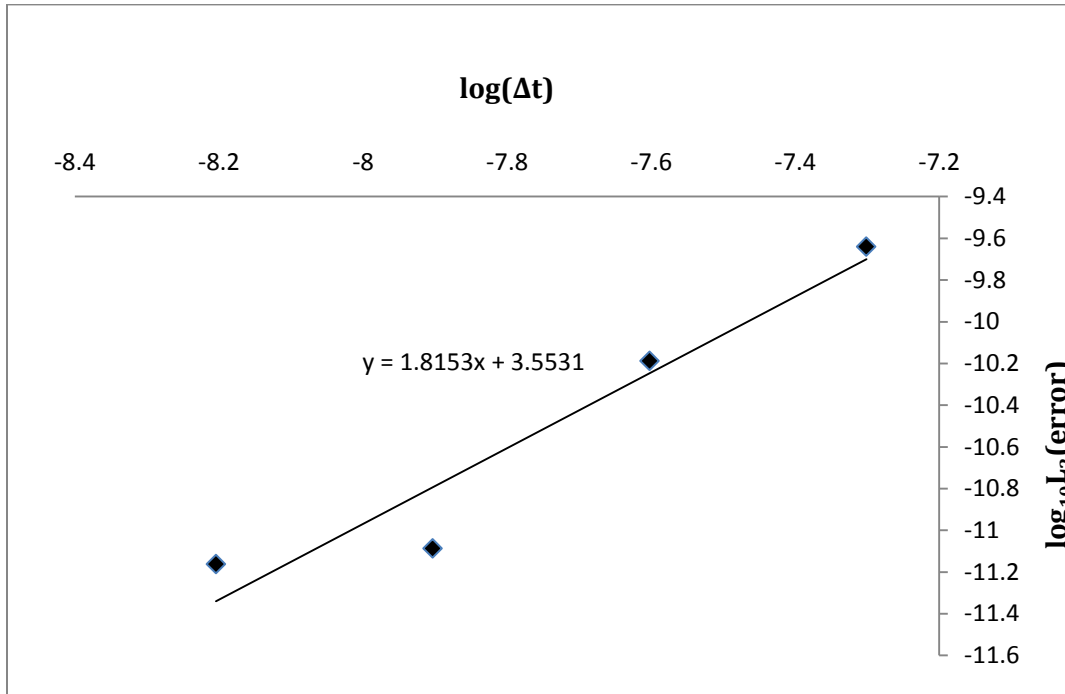**Figure 14: Convergence plot for surface flux**

Figure 15: Temporal convergence plot for surface displacement

From table 1, figure 14, and figure 15, it is clear that we observe a convergence order of 1.98 for the neutron flux, and of 1.82 for the displacement. Thus we get near second order convergence.

Chapter 5: Summary and Future Work

In this study, we have extended the IMEX algorithm (Kadioglu et al., 2011) for FBR modeling to incorporate transport effects. First, we demonstrated that the use of the diffusion model is inadequate for modeling a small FBR system. Because of the difference in flux profile and the difference in the PDE characteristics (hyperbolic transport equation vs. parabolic diffusion equation), we observe a significant difference in the transient behavior of the two neutronics models.

In order to incorporate transport effects into the IMEX algorithm, we utilized the moment-based acceleration method (Smith et al., 2002), (Knoll et al., 2011). When the moment-based acceleration method is used in the context of "tightly coupled" multiphysics simulation, the discretely consistent LO system, based on scalar flux, can be used to couple seamlessly to other physics. On the other hand, the original HO transport equation can be separated from the coupled system. This isolation of the transport system helps to mitigate the difficulty of having a prohibitively large number of unknowns in the nonlinear system. In addition, we have demonstrated second order convergence in the coupled simulation with the combination of the moment-based acceleration concept and the IMEX algorithm.

Several further studies are warranted. First, the combination of the simplified physical model and the IMEX algorithm used in this study has simplified physics coupling. More complex nonlinear systems should be considered in order to fully test the applicability and efficiency gain of the moment-based, scale-bridging concept. Furthermore, it is of interest to further minimize computational effort during transient calculations. For instance, a similar use of the moment-based acceleration method for thermal radiative transfer in (Park et al., 2013) has demonstrated an efficient predictor-corrector algorithm, which uses a single transport sweep per time-step. This

kind of more sophisticated time-stepping may be desired when we extend the study to larger multiphysics, multidimensional problems.

References

[1] E. Shabalin. Fast Pulsed and Burst Reactors. Pergamon Press (1979).

[2] D. Burgreen, Thermoelastic Dynamics of Rods, Thin Shells, and Solid Spheres. Nuclear Science and Engineering: 12, 203 – 217 (1962).

[3] S. Kadioglu, D. Knoll, and C. de Oliveira, "Multi-physics Analysis of Spherical Fast Burst Reactors", Nuclear Science and Engineering: 163, 1-12, March 2009.

[4] M. L. Adams and E. W. Larsen, "Fast Iterative Methods for Discrete-Ordinates Particle Transport Calculations," Progress in Nuclear Energy, **40**, No. 1, 3-159 (2002).

[5] Kopp H. J. (1963), "Synthetic Method Solution of the Transport Equation," Nuclear Science and Engineering, **17**, 65.

[6] Lebedev V. I. (1967), "An Iterative KP Method," USSR *Comp. Math and Math. Phys.* **7**, 1250.

[7] Marchuk G. I. and Levedev (1986) *Numerical Methods in Theory of Neutron Transport,* Second Revised Edition, Harwood Academic Publishers, London.

[8] Lebedev V. I. (1964), "The Iterative KP Method for the Kinetic Equation," *Proc. Conf on Mathematical Methods for Solution of Nuclear Physics Problems,* Nov. 17-20, 1964, Dubna, 93.

[9] Gelbard E. M. and Hageman L. A. (1969) "Convergence of Some Approximate Methods for Solving the Transport Equation," *Nucl. Sci. Eng.* **37**, 288.

[10] Reed W. H. (1971) "The Effectiveness of Acceleration Techniques for Iterative Methods in Transport Theory," *Nucl. Sci. Eng.* **45**, 245.

[11] Alcouffe R. E. (1976) "A Stable Diffusion Synthetic Acceleration Method for Neutron Transport Iterations," *Nucl. Sci. Eng.* **45**, 245.

[12] Gol'din V. Ya. (1967) "Quasi-Diffusion Method for Solving the Transport Equation," *USSR Comp. Math. and Math. Phys.* **4**, 136.

[13] Anistratov D. Y. and Larsen E. W. (1996) "Weighted Alpha Acceleration Methods for the Transport Equation," *Trans. Am. Nucl. Soc.* **75,** 154.

[14] Larsen E. W. (1990) "Transport Acceleration Methods and Two Level Multigrid Algorithms" *Modern Mathematical Methods in Transport Theory (Operator Theory: Advances and Applications, Vol 51)*, W. Greenberg and J Polewczak, eds, Birkhauser Verlag, Basel, **34**.

[15] Nowak P. F., Larsen E. W., and Martin W. R. (1987) "Multigrid Methods for S_N Problems," *Trans. Am. Nucl. Soc.* **55**, 355.

[16] Nowak P. F., Larsen E. W., and Martin W. R. (1988) "Multigrid Methods for S_N Calculations in X-Y Geometry," *Trans. Am. Nucl. Soc.* **56**, 291.

[17] Barnett A., Morel J. E., Harris D. R. (1989) "A Multigrid Acceleration for 1-D S_N Equations with Anisotropic Scattering," *Nucl. Sci. Eng.,* **102**, 1.

[18] Ramone G. L., Larsen E. W., and Martin W. R. (1997) " A Synthetic Acceleration Method for Transport Iterations," *Nucl. Sci. Eng.,* **125**, 257.

[19] Lewis E. E. and Miller W. F. Jr. (1976) "A comparison of P_1 Synthetic Acceleration Techniques," *Trans. Am. Nucl. Soc.* **23**, 202.

[20] Smith K. S. and Rhodes J. D. III (2000) "Casmo-4 Characteristics Methods for Two Dimensional PWR and BWR Core Calculations," *Trans. Am. Nucl. Soc.* **83**, 294.

[21] Seker V., Thomas J. W., Downer T. J. (2007) "Reactor Simulation with Coupled Monte Carlo and Computational Fluid Dynamics," *Joint International Topical Meeting on Mathematics & Computation and Supercomputing in Nuclear Applications Am. Nucl. Soc.*, Monterey.

[22] Procasini R., Chand K., Clouse C., Ferencz R., Grandy J., Henshaw W., Kramer K., Parsons D. (2007) "OSIRIS: A Modern, High Performance, Coupled, Multiphysics Code for Nuclear Reactor Core Analysis," *Joint International Topical Meeting on Mathematics & Computation and Supercomputing in Nuclear Applications Am. Nucl. Soc.*, Monterey.

[23] Lockwood B. A. (2007) "A Two Dimensional Fluid Dynamics Solver for Use in Multiphysics Simulation of Gas Cooled Reactors," PhD. Dissertation, Georgia Institute of Technology, Atlanta.

[24] McTaggart M. H. (1969) "Fast Burst Reactor Kinetics," *Proceedings of National Topical Meeting on Fast Burst Reactors*, Albuquerque.

[25] Reuscher J. A. (1969) "Thermomechanical Analysis of Fast Burst Reactors," *Proceedings of National Topical Meeting on Fast Burst Reactors*, Albuquerque.

[26] Hetrick D. L., Kimpland R. H., and Kornreich D. E. (1994) "Computer Simulations of Homogeneous Water Solution Pulse Reactors and Criticality Accidents," *Proceedings of National Topical Meeting on Physics, Safety and Applications of Pulsed Reactors*, Washington D. C.

[27] Pasternoster R., Kimpland R. H., Jaegers P., and McGhee J. (1994) "Coupled Hydro-Neutronic Calculations for Fast Burst Reactor Analysis," *Proceedings of National Topical Meeting on Physics, Safety and Applications of Pulsed Reactors*, Washington D. C.

[28] Wilson S. C., Beigalski S. R., and Coats R. L. (2007) "Computational Modeling of Coupled Thermomechanical and Neutron Transport Behavior in Godiva like Nuclear Assemblies," *Nucl. Sci. Eng.* **157**, 344.

[29] Green T. C. (2008) "Simulation of Reactor Pulses in Fast Burst and Externally Driven Assembliesm," PhD Dissertation, University of Texas, Austin.

[30] Tamang, A, and Anistratov, D. (2013) "A Multilevel Method for Coupling the Neutron Kinetics and Heat Transfer Equation," *SIAM Journal of Scientific Computations*, **19**, 266.

[31] Williamson, R. L., Hales, J. D, Novascone, S.R., Tonks, M. R., Gaston, D. R. Permann, C. J., Andrs, D., and Martineau, R. C. (2012) "Multidimensional Multiphysics Simulation of Nuclear Fuel Behavior," *Journal of Nuclear Materials*, **423**, 149.

[32] C. T. Kelley, Solving Nonlinear Equations with Newton's Method, SIAM (2003).

[33] G. Bell, and S. Glasstone, Nuclear Reactor Theory, New York: Von Nostrand Reinhold Company, 1979. Print.

[34] K. Smith, J. Rhodes III, Full core, 2D LWR core calculations with CASMO-4E, 2002, PHYSOR 2002, Seoul, Korea"

[35] H. Park, D. A. Knoll, and C. K. Newman, Nonlinear Acceleration of Transport Criticality Problems. Nuclear Science and Engineering, 171, pp. 1-14 (2012).

[36] D. Knoll, H. Park, K. Smith, Application of the Jacobian-free Newton-Krylov method to non-linear acceleration of transport source iteration in slab geometry. Nuclear Science and Engineering: 167, 122-132 (2011).

[37] D. E. Keyes, L. C. McInnes, C. Woodward, W. D. Gropp, E. Myra, M. Pernice. Multiphysics Simulations: Challenges and Opportunities. International Journal of High Performance Computing Applications (2012).

[38] H. Park, D. A. Knoll, R. M. Rauenzahn, C. K. Newman, J. D. Densmore, A. B. Wollaber, An efficient and time accurate, moment-based scale-bridging algorithm for thermal radiative transfer problems. SIAM Journal on Scientific Computing 35, S18-S41 (2013).

[39] E. Lewis, and W. Miller, Computational Methods for Neutron Transport, La Grange Park: American Nuclear Society, 1993. Print.

[40] Prinja A. K., and Larsen, E. W., Principles of Neutron Transport, Handbook of Nuclear Engineering, D. G. Cacuci (Ed.), Springer (2010).

[41] K. M. Singh (2014), Computational Fluid Dynamics, IIT Roorkee, India.